






Article

Otolith Analyses Highlight Morpho-Functional Differences of Three Species of Mullet (Mugilidae) from Transitional Water

Claudio D'Iglio ^{1,2,†}, Sabrina Natale ^{1,†}, Marco Albano ¹, Serena Savoca ^{3,*}, Sergio Famulari ¹,
Claudio Gervasi ¹, Giovanni Lanteri ¹, Giuseppe Panarello ¹, Nunziacarla Spanò ^{2,3} and Gioele Capillo ^{2,4}

¹ Department of Chemical, Biological, Pharmaceutical and Environmental Sciences, University of Messina, Viale F. Stagno d'Alcontres 31, 98166 Messina, Italy; cladiglio@unime.it (C.D.); snatale@unime.it (S.N.); malbano@unime.it (M.A.); serfamulari@unime.it (S.F.); claudio.gervasi@unime.it (C.G.); giovanni.lanteri@unime.it (G.L.); gpanarello@unime.it (G.P.)

² Institute for Marine Biological Resources and Biotechnology (IRBIM), National Research Council, 98122 Messina, Italy; spano@unime.it (N.S.); gcapillo@unime.it (G.C.)

³ Department of Biomedical, Dental and Morphological and Functional Imaging, University of Messina, Via Consolare Valeria, 98166 Messina, Italy

⁴ Department of Veterinary Sciences, University of Messina, Viale Dell'annunziata, 98168 Messina, Italy

* Correspondence: ssavoca@unime.it

† These authors contributed equally to this work.

Abstract: Otoliths are used in taxonomy and ichthyology as they can provide a wide range of information about specimens. They are an essential tool to monitor the most sensitive species for a sustainable exploitation level. Despite the increasing use of sagittae in research, their inter- and intra-specific variability and eco-functionality are still poorly explored. This paper aims to investigate the inter- and intra-specific variability of Mugilidae sagittae using morphological and morphometrical analysis, as well as scanning electron microscopy and shape analysis. The sagittae of 74 specimens belonging to three different Mugilidae species, collected from a coastal lagoon, were analyzed to give an accurate description of their morphology, morphometry, shape and crystalline habits. The results highlighted the intra- and inter-specific variability of sagittae, showing morphometrical differences among species and slight differences between left and right sagittae in *C. labrosus* individuals. Moreover, SEM images showed a peculiar crystal organization, with several different crystal habits and polymorphs. This study provides an accurate description of sagittae in the studied species, deepening the knowledge on inter- and intra-specific variations and crystal habits and providing data which will be useful for future studies on otoliths. With this data, it will be possible to improve conservation and exploitation sustainability in sensitive habitats.

Keywords: sagittae; Mugilidae otoliths; fish biology; SEM imaging; shape analysis



Citation: D'Iglio, C.; Natale, S.; Albano, M.; Savoca, S.; Famulari, S.; Gervasi, C.; Lanteri, G.; Panarello, G.; Spanò, N.; Capillo, G. Otolith Analyses Highlight Morpho-Functional Differences of Three Species of Mullet (Mugilidae) from Transitional Water. *Sustainability* **2022**, *14*, 398. <https://doi.org/10.3390/su14010398>

Academic Editor: Mario D'Amico

Received: 15 November 2021

Accepted: 18 December 2021

Published: 31 December 2021

Publisher's Note: MDPI stays neutral with regard to jurisdictional claims in published maps and institutional affiliations.



Copyright: © 2021 by the authors. Licensee MDPI, Basel, Switzerland. This article is an open access article distributed under the terms and conditions of the Creative Commons Attribution (CC BY) license (<https://creativecommons.org/licenses/by/4.0/>).

1. Introduction

Otoliths are acellular biomineralized concretions of calcium carbonate and other minor elements (Na, Sr, K, S, N, Cl and P), generated on a protein matrix in vertebrates' inner ears. In teleosts, inner ears are multi-sensory, stato-acoustic organs [1] with basic vestibular and acoustic functions (e.g., balance and hearing). They are essential in the perception of angular acceleration (derived from head/body rotation), linear acceleration and sound [1–7]. Each inner ear is composed of three semicircular canals, three end organs, named ampullae, and three otolith organs (sacculus, utricle and lagena). Inside these are located three otoliths (or ear stones): sagitta, lapillus and asteriscus. Each otolith is surrounded by an otolithic membrane. The latter mediates the connection between the sensory epithelia (macula sacculi) and otoliths. The otolithic membrane, the macula sacculi and the otolith are considered the "otolithic apparatus", a single physiological and morphological entity. Once perceived, sound occurs in the lower part of inner ear (sacculus

and lagena), which is specialized in sound reception, while the upper part (consisting of the utricle and semicircular canals) controls equilibrium. The otolith acts as a transducer of acoustic and vestibular signals to the fish's nervous system, through the macula sacculi. In bony fish, it consists of a solid calcium carbonate concretion, normally in form of aragonite crystals, with a small percentage (from 0.2% to 10% of the entire otolith) of organic matter (otoline) and other inorganic salts, secreted by the labyrinth walls and associated with a protein matrix on which they are developed [8,9].

Otolith growth is continuous over the fish's entire life, showing a daily deposition of new materials [10] and a high purity. They are metabolically inert [11,12] and represent a source of information about an individual's life history and age, thus possessing a high time-keeping properties [12].

They are one of the most useful anatomical structures for various studies of fish, leading to many practical applications [1,13,14]. These are not limited to ichthyology, but include ecological studies of predator fish, and some aspects of paleontology, stratigraphy, archeology and zoogeography. The otolith's morphology, due to its high inter-specific variability, is used in taxonomy for species discrimination and, since it is one of the main fossil fish remains, in palaeoichthyology for the evaluation of the biodiversity and species composition of past teleosts [9,13–18]. The otolith's morphometry, shape and chemical composition are also essential in ecological studies for prey identification during stomach content analysis [19,20], in fisheries science for stock discrimination [21–26] and population age structures [27,28], in fisheries management for migration pattern evaluations [29,30] and also in defining the morphofunctional adaptations of teleosts to different environmental conditions.

Among otoliths, sagittae, or saccular otoliths, are the most studied, due to their dimensions and their high inter-specific morphological variability. They are usually the largest otolith, except in some otophysan species, such as *Arius felis* (Linnaeus, 1766) [31]. Therefore, the saccular otolith is widely used for age determination in most bony fish species. In the mesial face of the sagitta, there is a depression called the *sulcus acusticus*, by which it is linked to macula sacculi. The *sulcus acusticus* is made up of two areas, ostium (anterior) and cauda (posterior), connected to each other by the collum. The morphological features, shape and crystalline structure of the *sulcus acusticus* have increasingly been used as a tool in stock assessment, species identification and ecological studies, analyzing their intra- and inter-specific variability in relation to environmental factors and ecological behavior of the species [32]. In fish, the size, shape and structure of sagittae vary ontogenetically, as well as from species to species and even between different populations of the same species. For this reason, it can be used in species discrimination and population studies [33–36].

The Mugilidae family, to which the species generally known as mullets belong, represents a large taxon of coastal marine fish, with a worldwide distribution that includes temperate, subtropical and tropical seas. Due to their tolerance to a wide range of salinities, they not only inhabit coastal marine waters, but also spend part of their life cycle in coastal lagoons, lakes and/or rivers. Mulletts, after their periods of rest and maturation in transitional environments (coastal lagoons, estuaries), perform a reproductive migration towards the sea; after spawning, some of them return to estuaries while others remain in marine waters [37–40]. The Mugilidae family includes 17 genera and approximately 72 species [41]. The Mediterranean Sea is inhabited only by eight of these species, all of which originally belonged to the same Genus: *Mugil*. Later, these were subdivided into four Genera: *Mugil*, *Liza*, *Chelon* and *Oedalechilus* [42]. Taxonomical discrimination among these species can be complex due to their complicated internal anatomy and external morphology. They are of great importance for professional and artisanal fishing, being species of high commercial value, especially for their gonads. Mugilidae are fished both for food purposes (and also often for bait) [38,39,43–45] over almost the entire planet, and for aquaculture production [43,44]. They are farmed both in extensive systems, and in semi-intensive and intensive systems, often in polyculture with other species; however, the latter production system is still based on the collection of wild fries, as induced spawning it is not practiced commercially.

Despite otoliths (especially sagittae) being increasingly used in many research fields, it is not yet fully understood how differences detected in sagittae among several fish species and populations are related to ecological, environmental or habitat variations. For this reason, the present study aimed to investigate inter- and intra-specific variability within Mugilidae sagittae, analyzing and comparing their morphology, morphometry, shape and external textural organization among three selected species: golden grey mullet, *Chelon auratus* (Risso, 1810), thicklip grey mullet, *Chelon labrosus* (Risso, 1827) and boxlip mullet, *Oedalechilus labeo* (Cuvier, 1829). These three species are euryhaline and share similar habitats. They inhabit neritic environments, forming inshore schools and frequently entering brackish lagoons and estuaries. In freshwater, it is also common to find *C. labrosus* and less common to find *C. auratus* [45–47]. *O. labeo* is the least euryhaline species among them. It mainly inhabits marine environments; but, occasionally, it is found in coastal lagoons [48,49]. All three species also share a similar trophic position, with *C. auratus* exhibiting the most pronounced predatory feeding habit. It mainly feeds on small zoobenthic organisms and detritus and, occasionally, on insects and plankton, while the other two species alternate a vegetarian diet (e.g., benthic diatoms, epiphytic algae) with the consumption of small invertebrates [50–53].

Individuals belonging to the aforementioned species were collected from a peculiar Sicilian transitional basin (Ganzirri lagoon) in order to add new information about the eco-morphological adaptation of marine species to brackish and transitional environments, especially in a constantly monitored area such as the Ganzirri lagoon. This is a sensitive environment, exploited by human activities since ancient times, and it is very important for the biodiversity it hosts, being a nursery and a shelter area for many marine species.

Investigating the sagitta features of individuals collected from this area, this study aimed to monitor and improve the knowledge of these species for a sustainable exploitation level of habitats and stocks and in order to better manage conservation. In order to give an accurate description of the sagittae in the studied species, with morphometrical measurements and comparisons between the left and right sagitta, a shape analysis was performed with R software, and an SEM imaging evaluation of their microcrystalline structure, between and within the species, was also performed. This research fills a gap in the literature regarding the considered mullet species, highlighting intra- and inter-specific otolith variability. Moreover, variability in microcrystalline organization, detected through SEM imaging, provides useful reference data for future studies on the microchemical and crystal organization of otoliths, which are essential for population studies and for environmental variation monitoring in natural conditions. This research adds new information regarding sagitta eco-morphology, laying the foundations for further studies concerning their functionality, morphology and adaptive role in the lives of teleosts. Deepening this knowledge is also essential for conservation purposes—both for brackish habitats, which are very vulnerable, and, by adding new shape analysis data, for Mullet stocks, which are exploited worldwide.

2. Materials and Methods

2.1. Study Area

The study area is located in the north-eastern area of Sicily, Italy (38°15'57" N, 15°37'50" E) (Figure 1a), between the Tyrrhenian and the Ionian Sea [49,50]. This area is of particular ecological importance, being part of the extremely peculiar and characteristic habitats of the area around the Strait of Messina [51–53].

In particular, the sampling location, Ganzirri Lagoon, is a brackish pond continuously in communication with the Strait of Messina through the “Due Torri” and “Carmine” Channels and with Faro Lake through the Margi Channel [54,55] (Figure 1b). The water level of this basin is not stable, as it is affected daily by the Strait of Messina tidal currents that change every 6h regularly, raising and lowering the level of the lagoon water [53].

This basin covers a 0.33 km² area (maximum depth: ~7 m; water volume: ~106 m³). It extends parallel to the coast of the Strait of Messina for 1670 m in length, and it is 282 m at its maximum width, with an elongated form oriented in the SW-NE direction [50].

Ganzirri and Faro lagoons are “Assets of ethno-anthropological interest” (declaratory measure 1342/88) since they are seats of traditional working and productive activities related to shellfish farming (mussel and cockle farming). The Lagoon of Capo Peloro is also an Oriented Natural Reserve (ONR), established by the Sicilian Region [56], as well as a Site of Community Importance (SIC) [57] and a Special Protection Zone (ZPS) [58–63].

In Ganzirri lagoon, shellfish farming took place from the first half of the 1700s up to 1995. Subsequently, due to sporadic events of anthropogenic pollution and contamination by pathogenic prokaryotes from the nearby town, this activity was interrupted by competent authorities [59].



Figure 1. Location of the studied area (a,b); image of Ganzirri lake (c) with sampling point in blue.

2.2. Sampling

Samples were collected between March 2021 and June 2021, in Ganzirri Lagoon (38°15'33" N; 15° 36' 58" E) (Figure 1c). A total of 74 Mugilidae (31 *C. auratus*, 32 *C. labrosus* and 11 *O. labeo*) were caught using throwing nets, also known as sparrow hawks or “rezzaglio” (Autorizzazione n.1138/A del 15.03.2021). This is an ancient circular fishing net, tied to a rope in the center of the circle. Fish were sampled and transported to the

Experimental Fish Pathology Center (Centro di Ittiopatologia Sperimentale della Sicilia–CISS), Department of Veterinary Sciences University of Messina, Italy. The fish included in this paper were not part of an experiment; all samples were used for diagnostic purposes commissioned by fish farmers, aiming at fish disease control. For that reason, no ethical committee approval was needed, even though all animal handling was performed under the European and Italian guidelines on animal welfare. The conducted analysis does not fall within the provisions of Legislative Decree No. 26/2014, implementation of the European Directive 2010/63/EU of the European Parliament, as waste material was used for diagnostic purposes and was, therefore, not regulated by laws on animal testing.

Next, each specimen was identified using dichotomous keys [50,51,64,65], weighed and measured [60]. For species identification, the head morphology, which is the most useful anatomical part from a taxonomic point of view and is normally employed in any identification key of the mullet, was evaluated (Table 1) [50,51,64–66]. Although the head is often broad and flattened or slightly dorsally convex in mullets, a wide variation in relative shape and size can be observed among Mugilidae species. The positional relationships between different anatomical elements such as jaws, nostrils, lips, eyes, opercular and preorbital bones and jugular space and their shape and size generate a variety of information useful for taxonomic identification [50,51,64–66]. For a precise identification of the species, the number of spines and rays of paired and unpaired fins and the number of scales in the lateral series were also evaluated. These features can be observed on the left side of the specimens, from the scales located just behind the head. The number of spines varied from approximately 24 to nearly 63, although sometimes different species had the same number. To have a greater confirmation of the species, at the time of necropsy, the pyloric blinds were collected and counted. Normally the number varies within a certain range in specimens belonging to the same species. Pyloric blinds can vary from 3 to 48 but more commonly from 5 to 10, although it is common to find several species of the same genus with the same number of pyloric blinds.

Finally, pairs of sagittae were manually removed by auditory capsule dissection, cleaned from tissue with 3% H₂O₂ for 15 min and then washed with Milli-Q water and stored dry inside Eppendorf microtubes. Images of left and right sagittae were captured for each individual specimen by a Leica M205C stereomicroscope with a LEICA IC80 digital camera. Each sagitta was photographed twice, once with the inner face facing up and once with the external face facing up, using the longest axis to orient the images horizontally for external face photos and vertically for inner face photos, in accordance with the literature [31].

Table 1. Morphological characters of studied species used for taxonomical identification.

<i>Chelon auratus</i>	<i>Chelon labrosus</i>	<i>Oedalechilus labeo</i>
Presence of pure gold stain on the operculum	Absence of pure gold stain on the operculum	Absence of pure gold stain on the operculum
Oval jugular space	Jugular space very short, straight, delimiting a very narrow oval space	Jugular space very narrow and linear
Anal fin with 8–9 rays, without spiny rays closetogether	Anal fin with 8–9 rays, without spiny rays closetogether	First anal fin with 3 spiny rays closetogether and 11 soft rays
Scales on head not extending beyond eyes	Scales on head extending beyond the eyes	Scales on head extending beyond the eyes
Upper lip not deep, shorter than pupil	Upper lip very deep, larger than pupil, with 3–4 sets of papillae	Upper lip deeper than pupil with finelabial fold
Rudimentary adipose eyelid	Rudimentary adipose eyelid	Rudimentary adipose eyelid
Dorsal scales with a dimple	Dorsal scales with a short dimple	Dorsal scales without dimple
Space between the two nostrils devoid of scales	Space between the two nostrils with scales	Space between the two nostrils devoid of scales

2.3. Morphometrical Analysis

Using ImageJ (ImageJ 1.48p software, freely available at <https://imagej.nih.gov/ij/>) (accessed on 21 September 2021) [61], in accordance with the literature [17,32,35,67–69], otolith measurements were recorded: otolith length (OL, mm), otolith width (OW, mm), otolith perimeter (OP, mm), otolith surface (OS, mm²), sulcus perimeter (SP, mm), sulcus surface (SS, mm²), sulcus length (SL, mm), cauda length (CL, mm), cauda width (CW, mm), cauda perimeter (CP, mm), cauda surface (CS), ostium length (OSL, mm), ostium width (OSW, mm), ostium perimeter (OSP) and ostium surface (OSS). Afterwards, other otolith shape indices were calculated: circularity (P^2/A), rectangularity ($OS/(OL \times OW)$), aspect ratio (OW/OL ; %), the ratio of the otolith length to the total fish length (OL/TL), the percentage of the otolith surface occupied by the sulcus (SS/OS , %), the percentage of the sulcus length occupied by the cauda length (CL/SL , %) and the percentage of the sulcus length occupied by the ostium length (OSL/SL , %) (Tables 2 and 3).

Table 2. Morphometric mean values with standard deviation (SD) and range of *Chelon auratus* and *Oedalechilus labeo* individuals: OL (otolith length), OW (otolith width), OP (otolith perimeter), OS (otolith surface), SP (sulcus perimeter), SS (sulcus surface), SL (sulcus length), CL (cauda length), CW (cauda width), CP (cauda perimeter), CS (cauda surface), OSL (ostium length), OSW (ostial width), OSP (ostium perimeter), OSS (ostium surface), CI (circularity), RE (rectangularity), aspect ratio (OW/OL %), the ratio of otolith length to total fish length (OL/TL), percentage of the otolith surface occupied by the sulcus (SS/OS %), percentage of the sulcus length occupied by the cauda length (CL/SL %) and percentage of the sulcus length occupied by the ostium length (OSL/SL %).

Otolith Morphological Characters (mm-mm ²)	<i>Chelon auratus</i> Mean ± SD	<i>Chelon auratus</i> Min.–Max.	<i>Oedalechilus labeo</i> Mean ± SD	<i>Oedalechilus labeo</i> Min.–Max.
OL	6.82 ± 0.78	5.56–9.60	6.27 ± 0.81	5.27–7.43
OW	3.38 ± 0.27	2.97–4.24	3.27 ± 0.28	2.83–3.62
OP	17.32 ± 1.44	14.21–22.05	16.38 ± 2.39	13.46–20.45
OS	17.06 ± 2.38	12.71–26.01	15.48 ± 3.18	11.65–20.05
SP	14.72 ± 1.89	10.62–19.28	14.24 ± 2.18	10.54–16.95
SS	0.12 ± 0.01	0.08–0.16	0.11 ± 0.02	0.08–0.13
SL	6.35 ± 0.89	4.31–8.41	6.05 ± 1.09	4.15–7.36
CL	4.12 ± 0.71	2.47–5.92	3.72 ± 0.83	2.27–4.63
CW	1.08 ± 0.24	0.50–1.60	0.98 ± 0.23	0.57–1.40
CP	9.04 ± 1.54	5.69–12.34	8.29 ± 1.53	5.77–10.30
CS	0.07 ± 0.01	0.04–0.09	0.06 ± 0.01	0.04–0.08
OSL	2.23 ± 0.38	1.54–3.20	2.34 ± 0.47	1.69–3.16
OSW	1.24 ± 0.29	0.80–2.09	1.24 ± 0.17	1.00–1.45
OSP	5.69 ± 0.83	4.02–7.60	5.95 ± 1.01	4.75–7.93
OSS	0.04 ± 0.01	0.03–0.06	0.04 ± 0.01	0.04–0.06
OP ² /OS	17.65 ± 1.10	15.89–19.99	17.41 ± 1.73	15.55–20.93
OS/(OL × OW)	0.74 ± 0.04	0.52–0.78	0.75 ± 0.03	0.71–0.79
OW/OL %	49.88% ± 0.04	38.11%–57.50%	52.44% ± 0.03	46.97%–56.48%
OL/TL	0.04 ± 0.01	0.03–0.06	0.04 ± 0.01	0.02–0.05
SS/OS %	0.66% ± 0.001	0.42%–1.12%	0.72% ± 0.00	0.47%–1.02%
CL/SL %	64.76% ± 0.05	52.00%–71.66%	0.61 ± 0.06	0.53–0.69
OSL/SL %	35.24% ± 0.05	28.34%–48.00%	0.39 ± 0.06	0.31–0.47

Table 3. Morphometric mean values with standard deviation (SD) and range of right (R) and left (L) sagittae in *Chelon labrosus* individuals: OL (otolith length), OW (otolith width), OP (otolith perimeter), OS (otolith surface), SP (sulcus perimeter), SS (sulcus surface), SL (sulcus length), SW (sulcus width), CL (cauda length), CW (cauda width), CP (cauda perimeter), CS (cauda surface), OSL (ostium length), OSW (ostium width), OSP (ostium perimeter), OSS (ostium surface), CI (circularity), RE (rectangularity), aspect ratio (OW/OL %), the ratio of otolith length to total fish length (OL/TL), percentage of otolith surface occupied by the sulcus (SS/OS %), percentage of the sulcus length occupied by the cauda length (CL/SL %) and percentage of the sulcus length occupied by the ostium length (OSL/SL %). (R = right, L = left).

Otolith Morphological Characters (mm-mm ²)	<i>Chelon labrosus</i> Mean \pm SD. (L. otoliths)	<i>Chelon labrosus</i> Min.–Max (L. otoliths)	<i>Chelon labrosus</i> Mean \pm SD (R. otoliths)	<i>Chelon labrosus</i> Min.–Max. (R. otoliths)
OL	6.73 \pm 0.33	5.97–7.54	6.71 \pm 0.33	6.04–7.45
OW	3.52 \pm 0.19	3.24–4.00	3.48 \pm 0.15	3.21–3.88
OP	17.36 \pm 0.79	15.88–19.62	17.24 \pm 0.72	15.93–18.89
OS	18.21 \pm 1.44	15.98–21.64	17.91 \pm 1.47	15.67–22.05
SP	15.57 \pm 1.22	13.19–18.13	14.72 \pm 1.51	12.31–19.30
SS	0.12 \pm 0.01	0.10–0.13	0.11 \pm 0.01	0.09–0.14
SL	6.29 \pm 0.41	5.45–7.25	2.43 \pm 0.77	0.93–5.75
CL	4.21 \pm 0.39	3.39–4.80	1.18 \pm 0.52	0.84–3.67
CW	1.20 \pm 0.19	0.65–1.58	4.15 \pm 0.68	1.04–5.13
CP	9.78 \pm 1.05	7.58–11.68	9.51 \pm 1.15	6.99–13.44
CS	0.07 \pm 0.01	0.06–0.09	0.07 \pm 0.01	0.05–0.10
OSL	2.09 \pm 0.31	1.64–2.90	1.26 \pm 0.37	0.09–2.07
OSW	1.43 \pm 0.25	0.97–2.00	1.90 \pm 0.34	0.94–2.37
OSP	5.79 \pm 0.65	4.82–7.20	5.21 \pm 0.76	3.79–6.98
OSS	0.04 \pm 0.005	0.04–0.05	0.04 \pm 0.01	0.03–0.05
OP ² /OS	16.58 \pm 0.61	15.71–18.48	16.62 \pm 0.60	15.59–18.69
OS/(OL \times OW)	0.77 \pm 0.02	0.71–0.81	0.77 \pm 0.02	0.72–0.81
OW/OL %	52.43% \pm 0.03	48.43–59.70%	51.95% \pm 0.02	46.58%–55.80%
OL/TL	0.03 \pm 0.003	0.03–0.04	0.03 \pm 0.003	0.03–0.04
SS/OS %	0.64% \pm 0.001	0.48%–0.78%	0.61% \pm 0.00	0.46%–0.85%
CL/SL %	66.84% \pm 0.04	56.98%–74.49%	48.51% \pm 0.10	34.29%–90.46%
OSL/SL %	33.16% \pm 0.04	25.51%–43.02%	51.49% \pm 0.10	9.53%–65.71%

2.4. Otolith Shape Analysis

Analysis of otolith shapes was performed using shape R, an open-source software package that runs on the R platform (R Gui 4.0.5), globally used to study otolith shape variation among teleost populations and species [62]. A threshold pixel value of 0.05 (intensity threshold) was used to binarize sagittae images. Each extracted outline was coupled to a master list file enclosing information on analyzed specimens (e.g., fish length, weight and origin). Wavelet and Fourier coefficients were extracted and adjusted to define the allometric relationships with fish lengths. The graph shown in Figure 2 was obtained through wavelet coefficient, with a mean otolith shape comparison among analyzed species. Deviation from the otolith outline was used to estimate the quality of obtained wavelet and Fourier reconstruction. The value 15 was set as the maximum number of Fourier harmonics to be shown. Finally, a g-plots R package was used to obtain the graph shown in Figure 3, to evaluate how variation in the wavelet coefficients is dependent on the position along the outline.

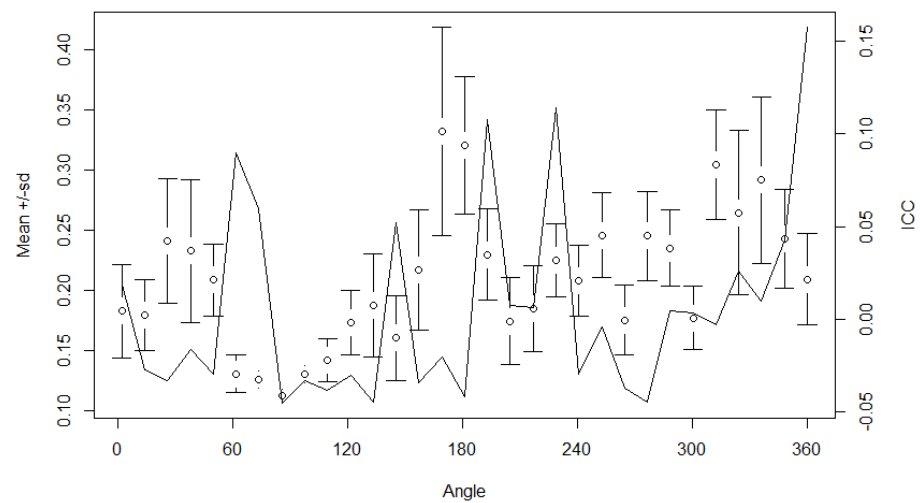


Figure 2. Mean and standard deviation (SD) of wavelet coefficients for all combined otoliths and the proportion of variance among species (black line). The horizontal axis shows angle in degrees ($^{\circ}$) based on the polar coordinates of mean shapes of left otolith contours. The centroid of the otolith is the centre point of polar coordinates.

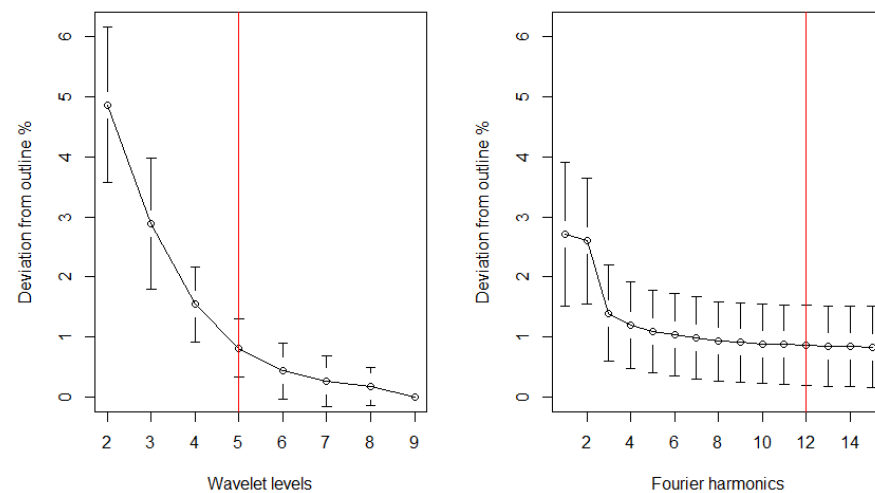


Figure 3. Plotting the quality of wavelet and Fourier outline reconstruction. The red lines indicate the level of wavelet and number of Fourier harmonics needed for a 98.5% accuracy of the remodelling.

2.5. SEM Analysis

A total of 9 otoliths were observed using SEM analysis, including 3 of *C. auratus*, 3 of *C. labrosus* and 3 of *O. labeo*. They were fixed for 48 h in 70% alcohol. Subsequently, samples were dehydrated in a graded series of alcohol from 70 to 100%, for 1 h in each solution. To avoid the critical drying point, samples were placed on a stub (SEM-PT-F-12) using conductive adhesive tables (G3347) and left for 12 h at 28 $^{\circ}$ C. Finally, the samples were sputter coated with 20 nm gold palladium. The samples were examined using a Zeiss EVO MA10 operating at the acceleration voltage of 20 Kv.

2.6. Data Analyses

All statistical analyses were conducted using Sigmaplot V.14, R vegan package V.2.5, and PAST V. 2.756 software.

Specific morphological parameters (OP2/OS, OS/[OL \times OW], OL/TL, OW/OL %, SS/OS %) were analyzed using a one-way analysis of variance (One-Way ANOVA) or Kruskal–Wallis one-way ANOVA to highlight any significant differences between the right and left sides of the otolith specimens within the same species. Differences in morphological

parameters between specimens of different species were also analyzed using one-way ANOVA or Kruskal–Wallis one-way ANOVA. Additionally, sulcus acusticus parameters were subjected to a linear discriminant analysis (LDA) to show differences between all the analyzed species.

Finally, the correlation between the measured parameters and fish weight and total length was tested using the Pearson correlation coefficient.

To determine differences in otolith contours, wavelet coefficients were used to analyze shape variation among species using an ANOVA-like permutation test. Moreover, shape coefficients were subjected to an LDA to obtain an overview of the differences in otolith shape between the species examined. The significance level was set at $p < 0.05$.

3. Results

3.1. Morphometric and Shape Analysis

As shown in Figures 4 and S1, the *C. auratus* specimens had a sagitta with rectangular or oblong shape, with an entire margin in the dorsal rim and lobed to the entire margins in the ventral rim. The anterior region was angled-round, with a short and pointed rostrum and an almost entirely absent anti-rostrum. The posterior region was flattened-round.

As shown in Figures 5 and S2, the *C. labrosus* specimens had a rectangular shaped sagitta, with crenate to irregular margins and irregular protuberances. The anterior region was angled-irregular, with a short and broad rostrum. The dorsal rim showed a marked plateau tilting towards the anterior rim. The anti-rostrum was absent or, in some specimens, poorly marked with a wide and small excisura. The posterior region was slightly irregular to round.

As shown in Figures 6 and S3, the *O. labeo* specimens' sagitta had a rectangular shape, with irregular margins in the dorsal and ventral rims. The anterior region was round to irregular, with a short and broad rostrum, and a short and pointed anti-rostrum.

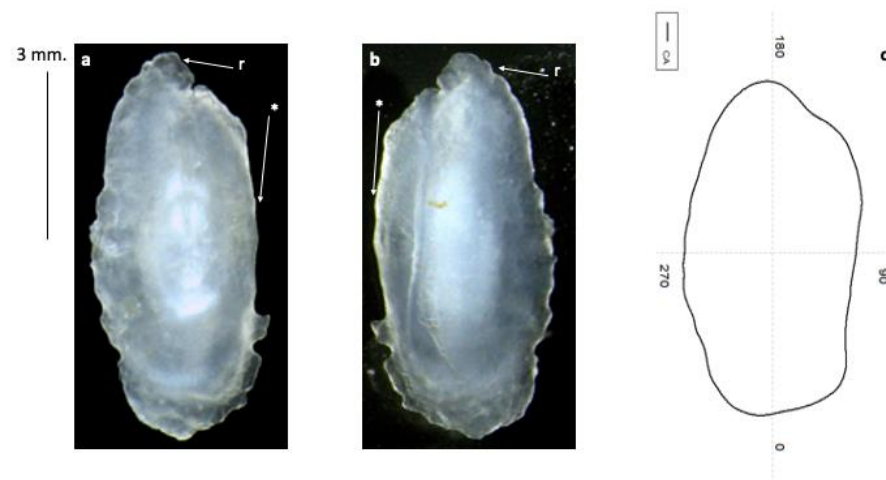


Figure 4. Left sagittae of *Chelon auratus* with scale bar. (a) Medial view; (b) lateral view; (c) mean shape; (r) indicates the rostrum, and (*) indicates the dorsal rim.

Concerning intra-specific differences (Table 4) among sagitta morphometrical parameters, in the specimens belonging to the *C. auratus* species, the correlation analysis revealed a moderate significant correlation between TL and SS/OS % ($\rho = 0.416$; $p = 0.001$). *C. labrosus* was the only species that showed differences between the right and left side of the otoliths, for the parameters CL/SL % ($H = 38.48$, $df 1$, $p < 0.001$) and OSL/SL % ($H = 38.48$, $df 1$, $p < 0.001$). Moreover, a significantly positive correlation was detected between TL and OW/OL ($\rho = 0.411$; $p = 0.001$), while a negative correlation was noted between TL and OL/TL ($\rho = -0.366$; $p = 0.0029$) and between BW and OL/TL ($\rho = -0.392$; $p = 0.001$). In *O. labeo* specimens a strong negative correlation was observed between TL and OL/TL ($\rho = -0.729$; $p = 0.001$) and between BW and OL/TL ($\rho = -0.658$; $p = 0.001$). A significant

positive correlation was recorded between TL and SS/OS % ($\rho = 0.561$; $p = 0.008$) and between BW and SS/OS % ($\rho = 0.499$; $p = 0.02$).

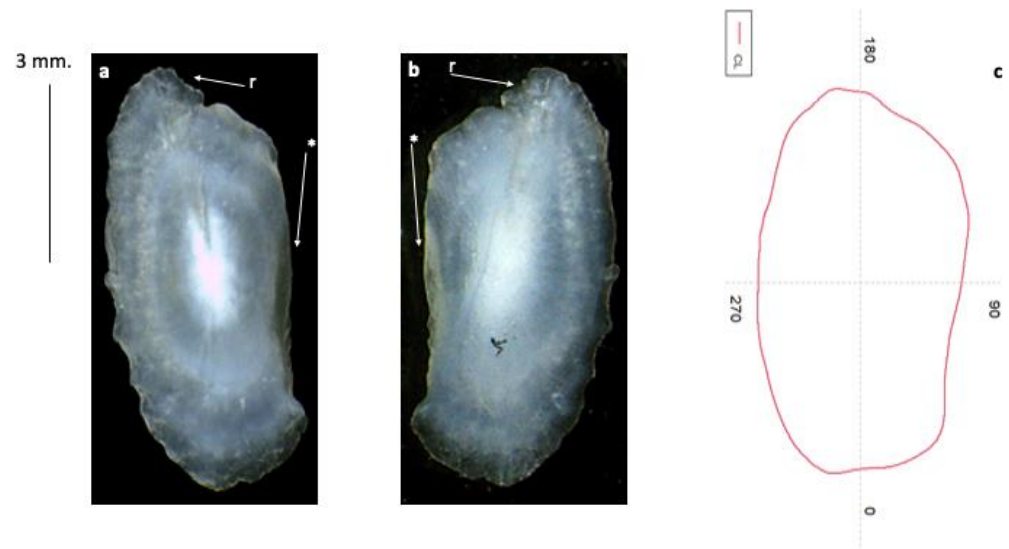


Figure 5. Left sagittae of *Chelon labrosus* with scale bar. (a) Medial view; (b) lateral view; (c) mean shape; (r) indicates the rostrum, and (*) indicates the dorsal rim.

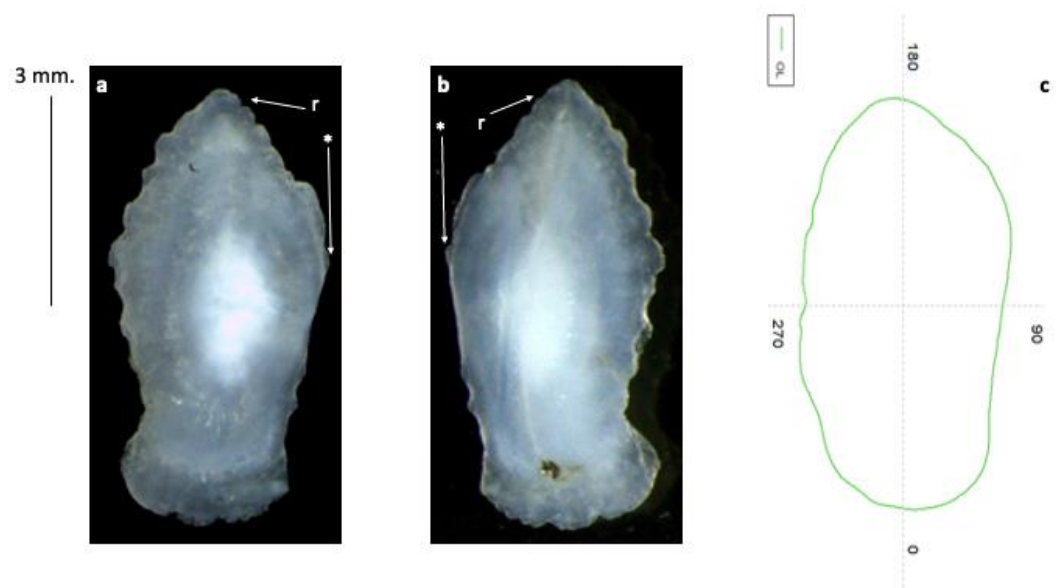


Figure 6. Left sagittae of *Oedalechius labeo* with scale bar. (a) Medial view; (b) lateral view; (c) mean shape; (r) indicates the rostrum, and (*) indicates the dorsal rim.

Concerning inter-specific differences among sagitta morphometrical parameters (Table 5), the investigated species showed significant differences in some parameters. *C. auratus* and *C. labrosus* showed differences in OP^2/OS ($H = 20.802$, $df2$, $p < 0.001$), $OS/[OLXOW]$ ($p = 0.001$), OW/OL % ($p < 0.002$) and OL/TL ($H = 12.477$, $df 2$, $p = 0.002$). *C. auratus* and *O. labeo* showed significant differences only in OW/OL % ($p = 0.014$). Finally, *C. labrosus* and *O. labeo* showed differences in $OS/[OLXOW]$ ($p = 0.012$).

As shown in the LDA plot (Figure 7), the first two axes showed a slight separation in the sulcus acusticus parameters between the three fish species analyzed.

The mean shape of otoliths differed significantly between the *C. auratus*, *C. labrosus* and *O. labeo* specimens ($p < 0.001$). The otolith contours are shown in Figure 8a. Marked differences in otolith shape have also been confirmed by LDA. From the LDA plot of the

first two discriminant functions, we can see that the three species were quite well separated (Figure 8b).

Table 4. Pearson Correlation results between total length, weight and selected morphometric parameters of *Chelon auratus*, *Chelon labrosus* and *Oedalechilus labeo*. Significant result was set at $p = 0.05$. OS (circularity), OS/(OL \times OW) (rectangularity), aspect ratio (OW/OL; %), the ratio of the otolith length to the total fish length (OL/TL), percentage of the otolith surface occupied by the sulcus (SS/OS, %), percentage of the sulcus length occupied by the cauda length (CL/SL, %) and percentage of the sulcus length occupied by the ostium length (OSL/SL, %). ns = not significant.

Fish Species	Morphometric Parameters	Weight		Total Length	
		ρ	p Value	ρ	p Value
<i>Chelon auratus</i>	OP ² /OS	ns	ns	ns	ns
	OS/(OL \times OW)	ns	ns	ns	ns
	OW/OL %	ns	ns	ns	ns
	OL/TL	ns	ns	ns	ns
	SS/OS %	ns	ns	0.416	0.001
	CL/SL %	ns	ns	ns	ns
	OSL/SL %	ns	ns	ns	ns
<i>Chelon labrosus</i>	OP ² /OS	ns	ns	ns	ns
	OS/(OL \times OW)	ns	ns	ns	ns
	OW/OL %	ns	ns	0.411	0.001
	OL/TL	−0.392	0.001	−0.366	0.0029
	SS/OS %	ns	ns	ns	ns
	CL/SL %	ns	ns	ns	ns
	OSL/SL %	ns	ns	ns	ns
<i>Oedalechilus labeo</i>	OP ² /OS	ns	ns	ns	ns
	OS/(OL \times OW)	ns	ns	ns	ns
	OW/OL %	ns	ns	ns	ns
	OL/TL	−0.658	0.001	−0.729	0.001
	SS/OS %	0.499	0.02	0.561	0.008
	CL/SL %	ns	ns	ns	ns
	OSL/SL %	ns	ns	ns	ns

Table 5. Results of t-test and ANOVA carried out on selected morphometric parameters between left and right sagitta and among left sagittae of *Chelon auratus*, *Chelon labrosus* and *Oedalechilus labeo*. Significant result was set at $p = 0.05$. OP²/OS (circularity), OS/(OL \times OW) (rectangularity), aspect ratio (OW/OL; %), the ratio of the otolith length to the total fish length (OL/TL), percentage of the otolith surface occupied by the sulcus (SS/OS, %), percentage of the sulcus length occupied by the cauda length (CL/SL, %) and percentage of the sulcus length occupied by the ostium length (OSL/SL, %). ns = not significant.

	OP ² /OS	OS/(OL \times OW)	OW/OL %	OL/TL	SS/OS %	CL/SL %	OSL/SL %
Comparison between							
L and R otoliths:							
<i>Chelon auratus</i>	ns	ns	ns	ns	ns	ns	ns
<i>Chelon labrosus</i>	ns	ns	ns	ns	ns	$p < 0.001$	$p < 0.001$
<i>Oedalechilus labeo</i>	ns	ns	ns	ns	ns	ns	ns
Comparison between species:							
<i>Chelon auratus</i> vs. <i>Chelon labrosus</i>	$p < 0.001$	$p = 0.001$	$p < 0.002$	$p = 0.002$	ns	ns	ns
<i>Chelon auratus</i> vs. <i>Oedalechilus labeo</i>	ns	ns	$p = 0.014$	ns	ns	ns	ns
<i>Chelon labrosus</i> vs. <i>Oedalechilus labeo</i>	ns	$p = 0.012$	ns	ns	ns	ns	ns

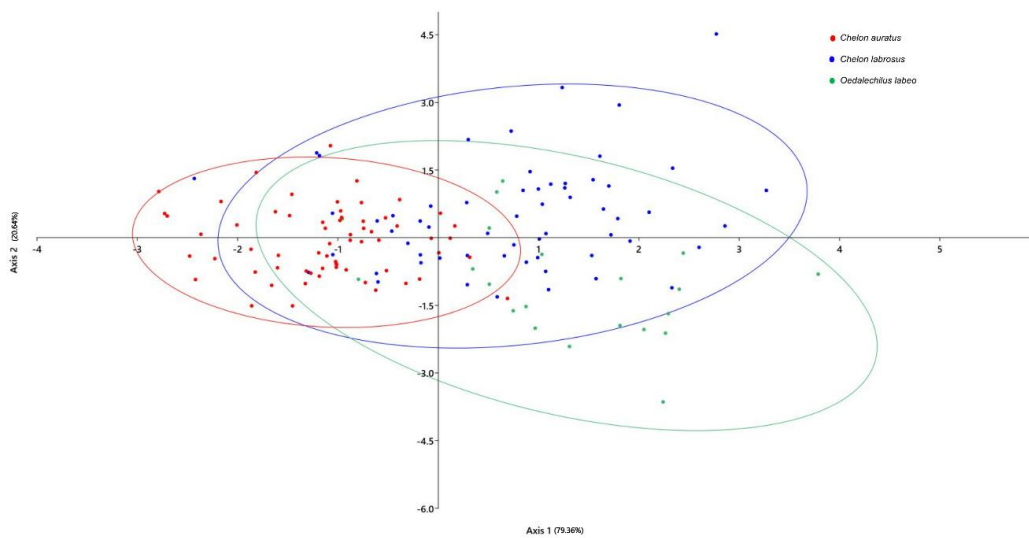


Figure 7. Linear Discriminant Analysis (LDA) of the sulcus acusticus computed between the species *Chelon auratus*, *Chelon labrosus* and *Oedalechilus labeo*. The LDA was based on selected sulcus acusticus parameters: sulcus acusticus area, sulcus acusticus perimeter, sulcus acusticus length, ostium area, ostium perimeter, ostium length, ostium width, cauda area, cauda perimeter, cauda length, cauda width, percentage of the otolith surface occupied by the sulcus (SS/OS, %), percentage of the sulcus length occupied by the cauda length (CL/SL, %) and percentage of the sulcus length occupied by the ostium length (OSL/SL, %). 95% probability ellipses are shown.

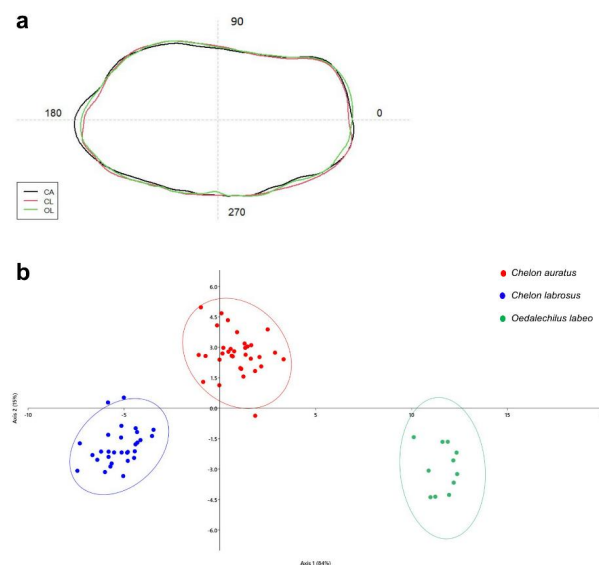


Figure 8. (a) Mean shapes of left otolith contours. CA is *Chelon auratus*, CL is *Chelon labrosus* and OE is *Oedalechilus labeo*. (b) Linear discriminant analysis plot between the species *Chelon auratus*, *Chelon labrosus* and *Oedalechilus labeo*, calculated on elliptic Fourier descriptors. Ellipses include 95% confidence interval.

3.2. Scanning Electron Microscopy (SEM) Analysis

Figure 9 gives an accurate sagittae view via SEM of the studied species. The sulcus acusticus was heterosulcoid with a suprmedian position and flat colliculi (homomorph) in all three species. The ostium was opened wide in the anterior margin and the cauda was distinctly closed away from the posterior margin (ostial mode opening). The ostium was tubular and curved in all the three species, with a more markedly curved shape in *C. labrosus* and *O. labeo* than *C. auratus* (Figure 9a–d). In this last species, the ostium was

funnel-like (Figure 9a), while in the other two species, it was more rectangular (Figure 9e,f). The anterior regions of the sagittae were peaked in all the studied species, with an absent or poorly developed anti-rostrum and a short and poorly pronounced rostrum, while the posterior regions were flattened and slightly oblique in some *C. auratus* specimens.

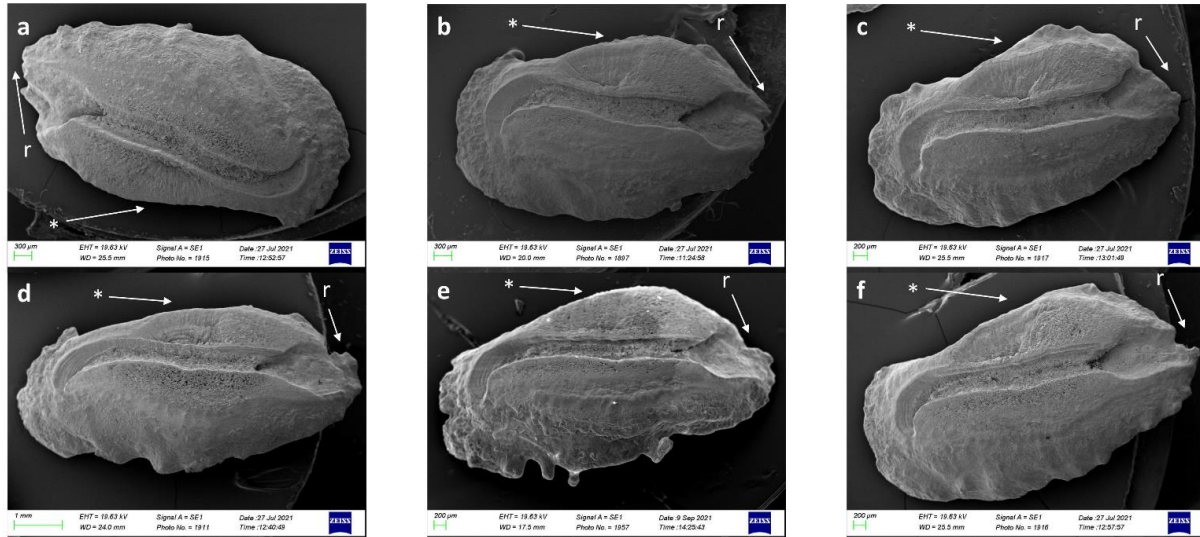


Figure 9. SEM imaging of the left sagittae proximal surface; (a–d) *Chelone auratus*; (b–e) *Chelone labrosus*; (c–f) *Oedalechilus labeo*; (r) indicates the rostrum, and (*) indicates the dorsal rim.

Concerning the external textural organization, SEM analysis highlighted a polymorph transformation, strictly related to the otoliths' mineralization process. All the analyzed sagittae showed radial oriented crystalline units, which had a chaotic orientation and were not equally sized (Figures 10a–e, 11a–c and 12a–c), probably due to the polymorph composition of the crystals. In all the studied species, the aragonite was found in two crystal habits (columnar habits and distinct plate habits) on the cauda surface with bigger, longer and narrower crystals (Figures 10d,e, 11b and 12c–e), while in the ostium, they were smaller and shorter than in the cauda, with a smooth surface (Figures 10b, 11d and 12b).

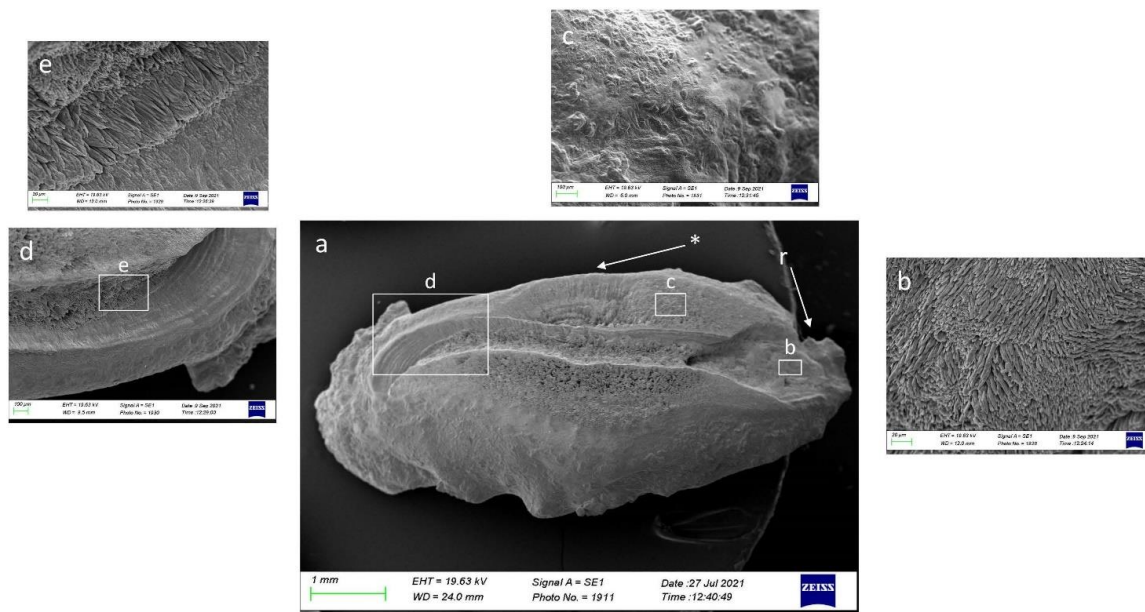


Figure 10. SEM imaging of left sagitta proximal surface in *Chelone auratus* (a), with details of external textural organization of ostium (b), area between cauda and dorsal rim (c) and cauda (d,e); (r) indicates the rostrum, and (*) indicates the dorsal rim.

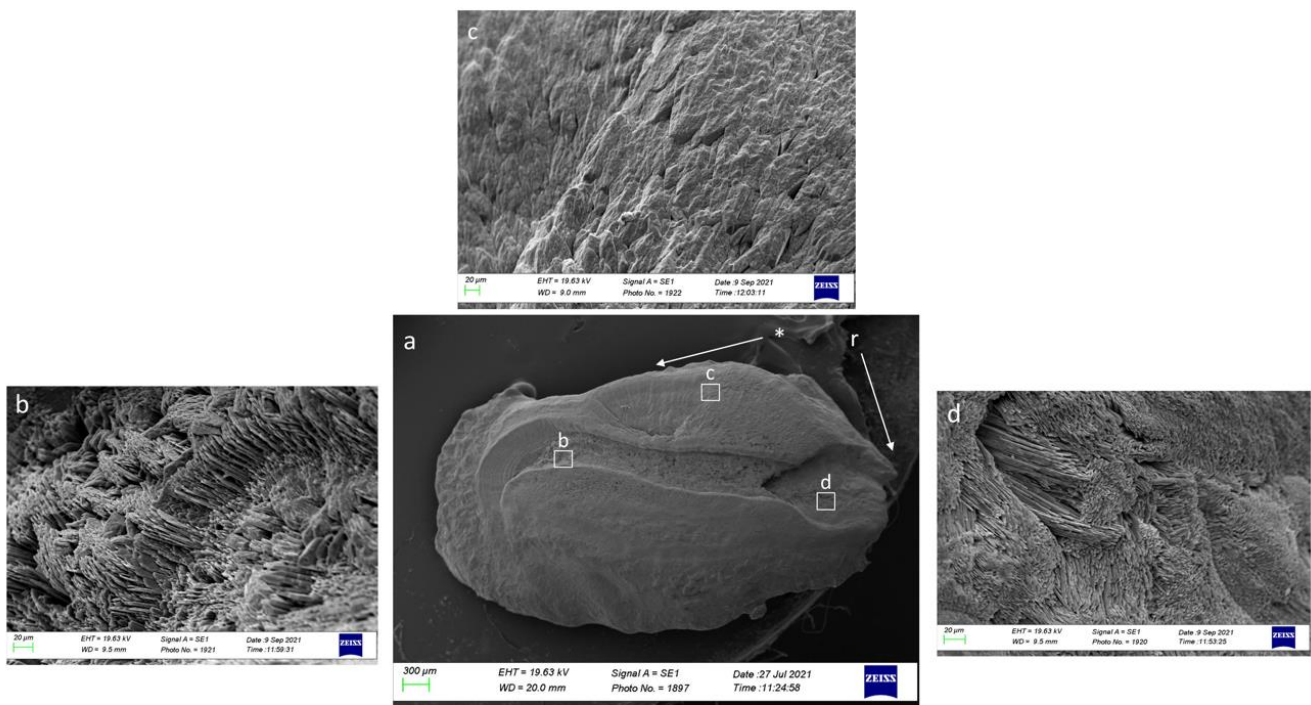


Figure 11. SEM imaging of left sagitta proximal surface in *Chelon labrosus* (a) with details of external textural organization of cauda (b), dorsal area (c) and ostium (d); (r) indicates the rostrum, and (*) indicates the dorsal rim.

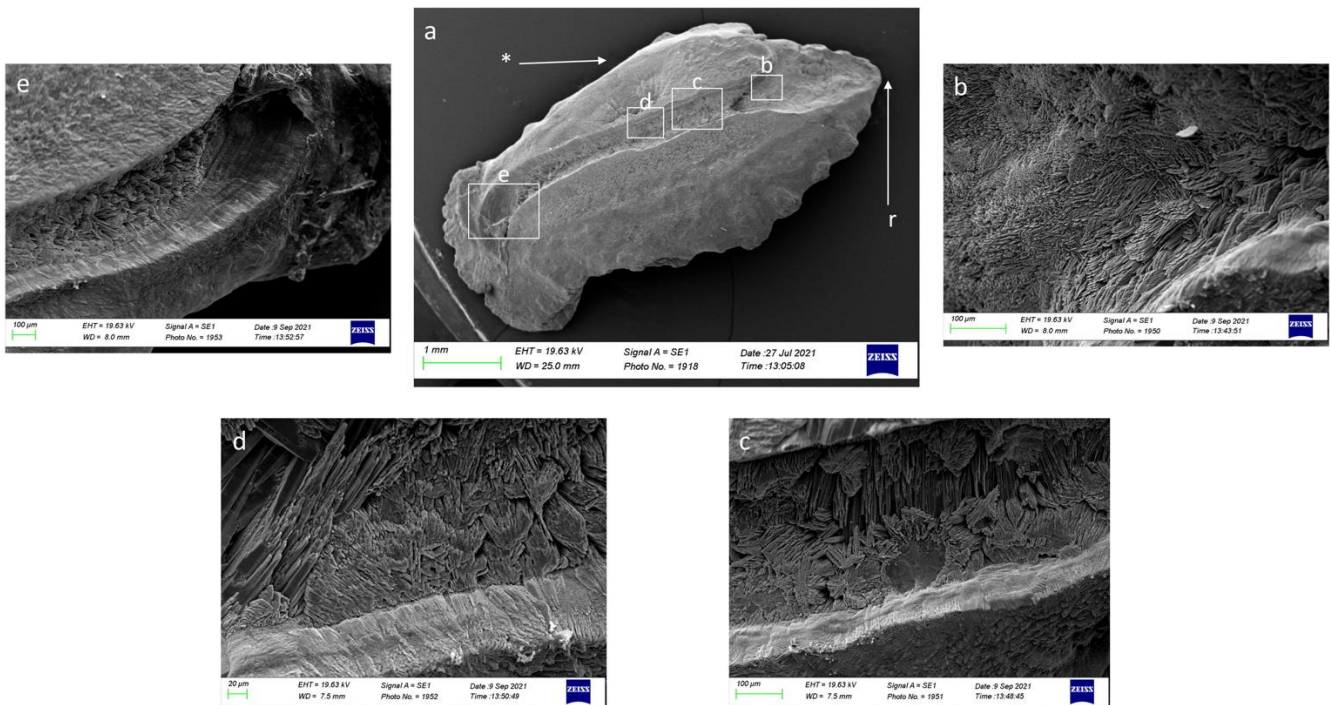


Figure 12. SEM imaging of left sagitta proximal surface in *Oedalechilus labeo* (a) with details of external textural organization of ostium (b) and cauda (c–e); (r) indicates the rostrum, and (*) indicates the dorsal rim.

Moreover, several polymorphs and habits of calcium carbonates were detected in many otoliths, especially of *C. labrosus*. These crystalline habits showed different shapes and organizations including small, locally oriented needles, long prisms and large rhombohedral

crystals. This last kind was detected on the *C. labrosus* sagitta surface (Figure 13a–h); the long prism shaped crystals (Figure 14a,c,e) and small, locally oriented needles (Figure 14b,d) were detected on the cauda surface of *O. labeo* and of *C. auratus*. SEM imaging also showed carbonate formations similar to “globular secretion” on the sagitta surface of *C. labrosus* (Figure 15a–c), along with evidence of large prismatic crystals (Figure 16a–d).

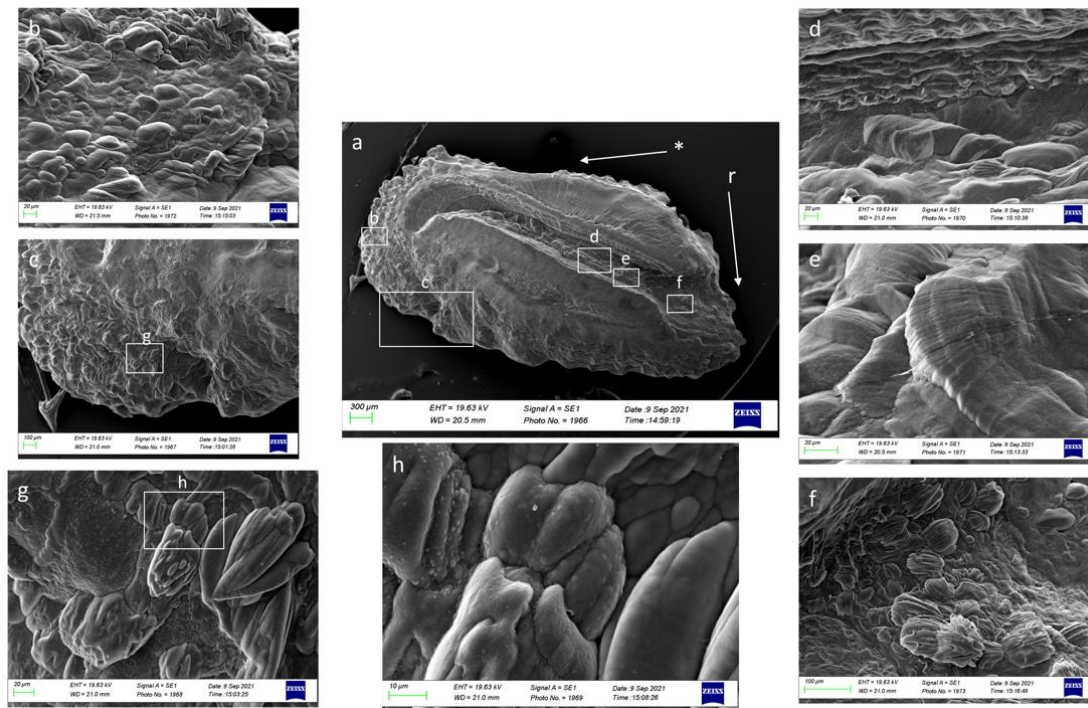


Figure 13. SEM imaging of left sagitta proximal surface in *Chelon labrosus* (a) with details of several calcium carbonate habits in posterior area (b), ventral area (c–h), cauda (d,e) and ostium (f); (r) indicates the rostrum, and (*) indicates the dorsal rim.

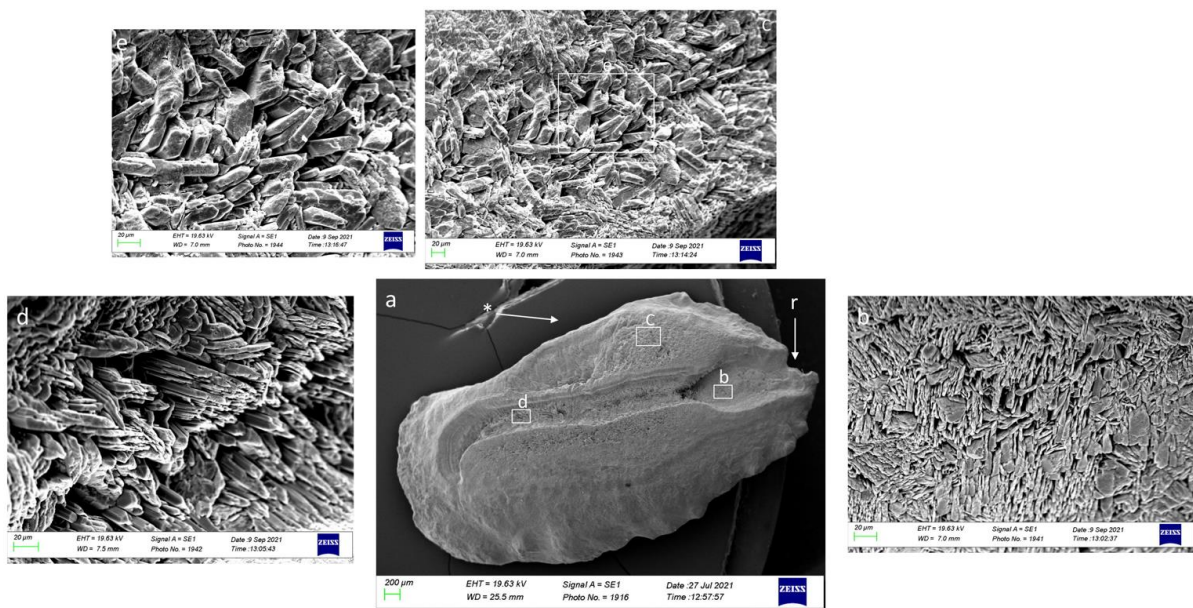


Figure 14. SEM imaging of left sagitta proximal surface in *Oedalechilus labeo* (a) with details of several calcium carbonate habits in ostium (b), dorsal area (c–e) and cauda (d); (r) indicates the rostrum, and (*) indicates the dorsal rim.

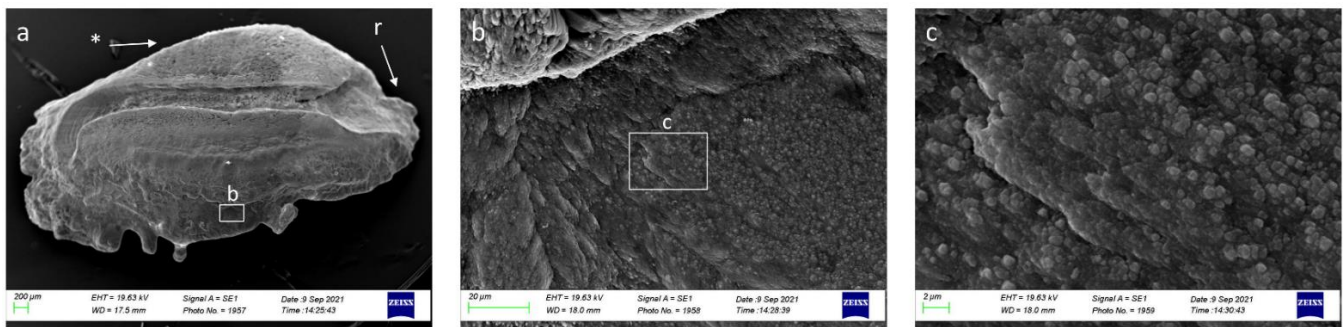


Figure 15. SEM imaging of left sagitta proximal surface in *Chelon labrosus* (a) with details of granular crystalline habit in ventral area (b,c); (r) indicates the rostrum, and (*) indicates the dorsal rim.

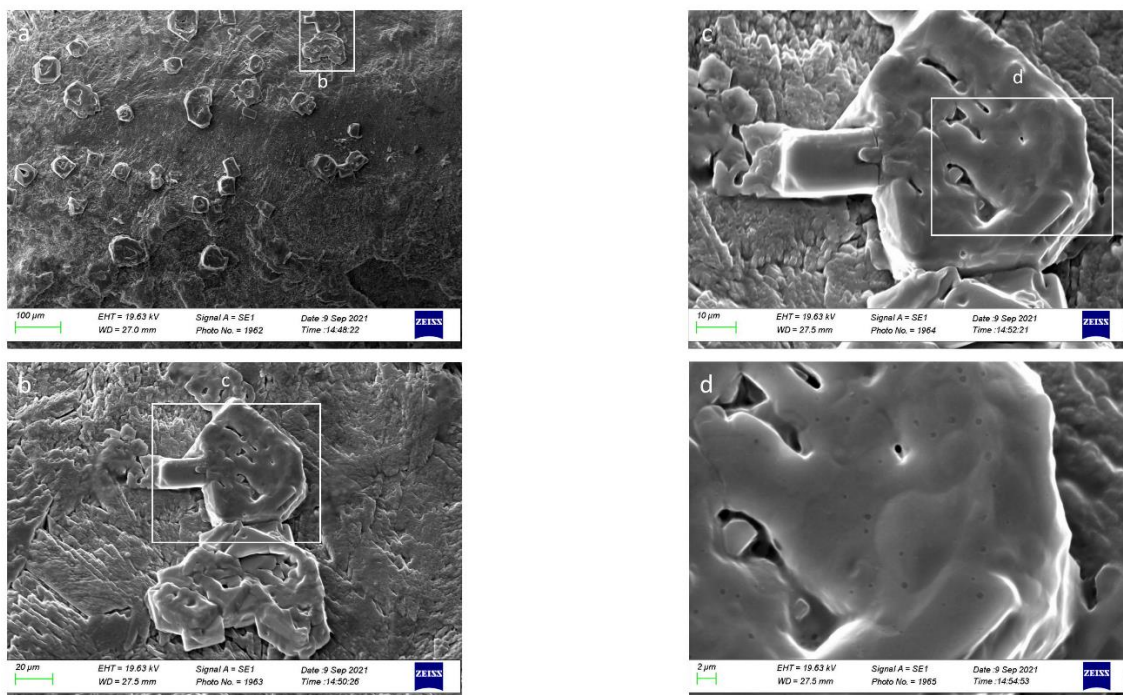


Figure 16. SEM imaging of large prismatic crystals in *Chelon labrosus* (a–d).

4. Discussion

The evaluation of intra-specific morphological differences among sagittae is essential to better understand otolith variability in relation to environmental factors and habitats. The morphological and shape variability of sagittae among populations from different geographical areas is at the base of stock assessment, and it has been demonstrated and thoroughly investigated by several authors [31,63–70]. Although the application of shape and morphological studies on wild populations are not enough to explain all the adaptive response of sagittae to environmental conditions or habitats, and common garden experiments are generally required, studies on otolith morphometry and morphology and the comparison among otoliths of different populations are essential to broaden knowledge on these differences and to help in detecting them.

Morphometrical results reported in the present study showed slightly morphological differences between the sagittae of Mugilidae species from the investigated area and those, described in the literature, from western Mediterranean Sea, northeastern Mediterranean Sea and Atlantic Ocean populations [17,42,71–80]. The *C. auratus* specimens from Ganzirri lagoon showed a more rectangular sagitta, with pronounced sagitta length to total fish length ratio and rectangularity values, and a lower circularity and sagitta aspect ratio than

those, reported by previous literature, from others geographical areas [17,42,79,80]. The margins of anterior region showed an accentuated regularity in the studied specimens compared to those from the northeastern Mediterranean Sea [71], while the rostrum was more pointed than those from the western Mediterranean Sea [15,72]. The positive correlation shown by statistical analysis confirmed the most pronounced sagitta dimension in the studied specimens. The positive correlation between ratio of sulcus acusticus surface to the entire sagitta and the increase in specimen size was probably related to an accentuated sulcus acusticus growth, which could depend on species ecology and its adaptation to the sampling area.

In addition, for *C. labrosus*, the morphology of the sagittae was different compared to those, shown by the literature, from the western Mediterranean and Atlantic Ocean [15]. The rectangularity was higher, while circularity was lower than data reported by previous literature [15], while the sagitta aspect ratio was the same, and the sagitta length to total fish length ratio was slightly higher. The irregular margins of the anterior region were similar to those observed in specimens from the northeastern Mediterranean Sea, western Mediterranean Sea and north Atlantic [17,71–80]. By contrast, the posterior region was flattened. Statistical analysis showed an accentuated increase in sagitta width, related to total fish length increase. This condition was also confirmed by the negative correlation observed between total fish length and the sagitta length to total fish length ratio. This was also the only species to show slight differences between left and right sagittae, especially on sulcus acusticus proportions (the cauda length to sulcus acusticus length ratio and the ostium length to sulcus acusticus length ratio). To the best of our knowledge, this is the first description of these differences in *C. labrosus* otoliths, confirming the peculiarity of specimens inhabiting Ganzirri lagoon. The detection of directional bilateral asymmetry is essential for stock assessment studies since it can affect otolith shape enough to be a potential new accurate method for stock identification [73,74]. Slight changes between left and right sagittae could be related to ecology (e.g., feeding strategy), and it is possible that the *C. labrosus* population from the studied area could show ecological features, related to habitat peculiarity, not found in other populations. Further analysis on specimens from Ganzirri lagoon are required to confirm this hypothesis.

To the best of our knowledge, this is also the first time in which *O. labeo* morphometrical parameters have been described. Regarding morphological aspects, the *O. labeo* specimens from the investigated area showed a rectangular sagitta, with regular rims in dorsal and ventral margins and an irregular anterior region different than those shown in the literature regarding the northeastern Atlantic and Mediterranean Sea [41]. The strong negative correlation observed between sagitta length and total fish length and weight showed an otolith dimension not directly related to those of the specimens. In contrast, the positive correlation between the sulcus acusticus surface to sagitta surface ratio and total fish length and weight confirmed a more accentuated increase in sulcus area than in the entire sagitta. These morphometrical features of the sagitta could be related to species lifestyle and life history. Further analysis of its ecology, migration patterns and key lifetime habitats are required to understand what might be related to these correlations.

All these differences in morphology detected between the studied fish species and populations from other geographical areas could lead to changes in sagittae between different stocks and they could be related to transitional environment peculiarities. It is difficult to find a direct correlation between environmental factors and variations in morphology and the morphometrical parameters of sagittae, but this kind of study broadens knowledge of the morphofunctionality of Mugilidae sagittae and their adaptation to different environmental factors. The results reported in the present paper confirm the great value of research on sagitta morphology in exploring the differences between different populations of the same species inhabiting different environments, highlighting the adaptation of teleosts to various habitats, as well as their features. Regarding Ganzirri lagoon, the particular water circulation affecting this transitional basin often generates a vertical gradient of nutrient stratifications, which determines consequences for the biogeochemical cycling of

nutrients and the anaerobic decomposition of organic matter [75]. Moreover, these also influence a vertical zonation of the planktonic microbial community of the basins. Water exchanges with the sea and underground springs, as well as meteorological and climatic conditions, influence the environmental characteristics of Ganzirri lagoon across seasons through large fluctuations in chemical-physical parameters, especially salinity, temperature and dissolved oxygen [76]. This kind of environmental factor fluctuation leads to adaptive behavioral and morphological responses, especially influencing otolith structure and composition [12,27,77–79], to a greater extent in fish that inhabit transitional waters than in fish that inhabit the open sea. According to the literature, salinity and temperature variations can influence the deposition rate of calcium carbonate, causing variations in sagitta polymorph percentage, crystal habits and, at the macroscopical level, morphological and shape variations too [80–83]. For this reason, Ganzirri lagoon features could lead to several variations among the sagittae of investigated species [12,32,34,73,84–92], confirming the importance of otoliths for eco-morphological and morphofunctional studies. Further analysis on feeding behavior and population dynamics is required to better understand the ecology of these three species in peculiar environments, such as the brackish lagoon considered in the present study.

The relatively few interspecific differences detected among the morphometrical parameters could be strictly related to the closeness at the taxonomic level of the studied species, since these belong to the same family and, in the case of *C. auratus* and *C. labrosus*, to the same genus [43]. Interspecific differences among otoliths, reported between the studied species, primarily concerned circularity, rectangularity, sagitta aspect ratio and the ratio of the sagitta length to the total fish length. All these differences were confirmed by the shape analysis. Indeed, *O. labeo* sagitta contours have clearly shown a stronger circularity than in those of the other species. A marked rectangular shape and longer sagitta were detected in *C. auratus*, which showed the highest otolith width compared with the other species analysed. This result has been confirmed by the highest values of sagitta aspect ratio and otolith length to total fish length ratio, compared to the other two species,

The *C. labrosus* specimens showed an intermediate sagitta morphology compared with the other two species, with a more pronounced rectangularity than *O. labeo* and a marked circularity compared to *C. auratus*. Concerning the sulcus acusticus parameters, the three Mugilidae species showed a similar morphology, as confirmed by LDA, with few differences. Indeed, the species share the same habitats and a similar ecological niche. Ecological differences with regard to the feeding habits—which in *C. auratus* are mainly those of a pelagic predator, while the other two species are herbivorous and benthic predators—could lead to the variation, although small, in sagittae morphology and shape between species, as reported by the previous literature on different species [32,33,35,73,88,93,94]. Further analysis of the feeding habits and diet of the studied species is required to confirm this hypothesis. Regarding the life cycles of the analyzed fish species, *O. labeo* has some differences compared to the other two. It is mainly a marine species; but it is common to find it in Ganzirri lagoon as well. It probably enters the brackish lagoon during the spawning period. The lagoon is a transition zone with high water trophism and low hydrodynamism, especially compared to the Strait of Messina waters. Because of these features, the study site represents a nursery area for many marine species and an optimal environment for feeding and protection against predators and the strong Strait of Messina currents. Further analysis of the ecology and life history traits of the studied species are required to better understand what drives the interspecific shape variations shown by the results. As reported in the previous literature on different species [28,34,64,84–89], the factors influencing sagittae shape diversity among species are manifold. They are mainly related to life history traits and ecological differences, highlighting how otoliths can reflect eco-morphological and morphofunctional adaptation to several habitats and lifestyles.

Moreover, our results have confirmed the effectiveness of interspecific variation among sagittae shape and morphology as a useful tool for discrimination among congeneric species, especially in a cryptic family such as Mugilidae. Indeed, discrimination of species

through taxonomic identification in this family is very difficult, due to high morphological similarities [40]. For this reason, molecular phylogenetic analysis provides essential information to understand the speciation mechanism of the Mugilidae family, as reported in the literature [42,90–92]. Interspecific morphological, morphometrical and shape differences among sagittae are another useful tool with which to discriminate among Mugilidae species. However, it is essential to consider the dual regulation which influence otolith growth and shape. Indeed, several studies have shown how environmental factors (e.g., water temperature and depth), species biology (e.g., year class, age, sex and stock) and genetics could influence the differences in otolith shape and morphology between stocks and species [23,93–96]. Further genetic analysis is required to understand the systematic relationship among studied species from Ganzirri lagoon and to evaluate the influence of genetics and environmental factors on otolith shape and morphology. This is essential for proper fisheries management and for all studies that involve such species with high commercial and ecological value.

The SEM imaging, performed in this study for the first time to investigate the sagittae external textural organization of *C. auratus*, *C. labrosus* and *O. labeo*, showed a very peculiar crystal organization.

SEM imaging analysis showed the presence of aragonitic crystals with various shapes (circular, hexagonal and lamellar forms) as described by previous research for other species [97]. As reported by a previous study on *Poecilia mexicana* (Steindachner, 1863) [98], large hexagonal crystals were detected in the sulcus acusticus of some *O. labeo* specimens (see Figure 12c,d). This peculiar crystalline habit was related to populations living in well-lit surface environments. Despite Ganzirri lagoon being a typical transitional environment, it is characterized by well-lit and oxygenated water for most of the year. In the *Acipenser brevirostrum* (Lesueur, 1818) specimens, these hexagonal crystals were described as calcite-like crystals [97]. The large rhombohedral crystals found in some *C. labrosus* specimens resembled those described in *Macruronus novaezelandiae* (Hector, 1871) as static calcitic crystals. Similar prismatic calcite crystals were also found in *Cilus gilberti*, (Abbott, 1899) and *Sciaena deliciosa* (Tschudi, 1846) specimens [99]. This carbonate habit was found in sulcus acusticus and near the posterior margin of *C. labrosus* specimens (see Figure 13b,d,e). Moreover, near the sagitta ventral margin, another peculiar crystal habit was detected (see Figure 13c,g,h), similar to those described in *Hoplostethus atlanticus* (Collett, 1889) as small granular vateritic crystals [97]. The large crystals found in *C. labrosus* (see Figure 16a–d) were like the calcium carbonate overgrowth observed by previous investigation on the otolith surface and in vitro crystallization experiments [100]. Moreover, the presence of on the sagitta surface of some specimens was also detected (see Figures 13h and 15b,c). These spherules, composed of several subunits, seemed to be similar to those described in *Encheliophis boraborensis* (Kaup, 1856) [101]. The spherules could be the layer of carbonate deposition, which give otoliths their globular surface. This globular carbonate deposition was similar to the calcium carbonate precipitate found on extracellular globules secreted by *Desulfonatronum lacustre* [102,103]. The endolymph proteins in teleosts' inner ears could induce carbonate precipitation, as seen in this bacterium [104], triggering the globular surface of otoliths with the presence of spherules, as shown in SEM images of the specimens analyzed in our study.

The presence of different crystal habits and of polymorphs with small locally oriented needles, long prism shapes, large rhombohedral crystals and globular secretion, especially in *C. labrosus* specimens, may be related to several environmental factors. Considering the Ganzirri lagoon, this is indeed a highly unstable environment close to the sea, with salinity fluctuation, which could influence the carbonate precipitation triggered by endolymph proteins and consequently the crystalline orientation and composition of otoliths, as reported in previous literature on other geographical area and species [1,11,12,31,34,105–115]. The presence of calcite and vaterite crystals and the several habits of different carbonate polymorphs are strictly related not only to environmental parameters, but also to individual pathological conditions and the species' ecological features, such as feeding habits,

as demonstrated by several authors [76,107,109,110,115]. Further analysis on the micro-chemical composition of sagittae is required to confirm the presence and the percentage of different carbonate polymorphs, investigating also how their occurrence is related to the environmental conditions and parameters of Ganzirri lagoon, or to species ecology or physiology. The continuous environmental parameter monitoring of this brackish lagoon offers a unique opportunity to find a correlation between crystalline variations in sagittae and the physico-chemical parameters of a natural environment. Understanding the morphological, morphometrical and microcrystalline structure variations in relation to transitional environmental conditions is essential to increase knowledge about teleost adaptation to several environmental factors and habitats and to the investigation of how sagittae variations are related to environmental parameters or anthropogenic activities. Indeed, the changes between populations might be caused by both ecomorphological adaptation to different environments and genetic differentiation.

This study has also created data that will be useful as reference data for future studies by means of which it will be possible to improve conservation and sustainable exploitation in sensitive habitats such as transitional water. An improved analysis and study of Mugilidae sagitta microchemistry and crystal composition will aid the comprehension of the coastal lagoon's role in stock maintenance as an essential environment associated with recruitment, settlement and spawning [82,105–108]. Therefore, improving the conservation of these sensitive environments, with sustainable stock and habitat exploitation, is essential for species protection and for the good functioning of the entire marine ecosystem [91,116–121].

5. Conclusions

The present study provides an accurate description of sagitta morphology, morphometry, shape and crystal habits in *C. labrosus*, *C. auratus* and *O. labeo*, deepening our knowledge of inter- and intra-specific variations. This kind of study is essential for a correct evaluation and subdivision of several species and stocks, especially for cryptic species, such as those belonging to the Mugilidae family, which are of high commercial value. Proper fisheries management is essential for their conservation, to guarantee a sustainable exploitation level in compliance with the environmental history and ecology of the species; for this purpose, thorough and accurate studies of the otoliths of each Mugilidae species are needed. To the best of our knowledge, this study reports the first description of the external textural organization of *C. labrosus*, *C. auratus* and *O. labeo* investigated using SEM imaging, and the first otolith shape and contour analysis performed with R software. Morphometrical analysis on *O. labeo* sagittae has never been carried out before, and this study adds new and important information to the knowledge base.

SEM images of the crystalline structure showed peculiar crystalline habits and polymorphs which could be related to several factors, such as environmental parameters and chemical features of Ganzirri lagoon, individuals' physiological conditions and species ecological features. This study confirmed that otolith capacity reflects environmental and other parameters; this should be reconfirmed by further analyses of the same and similar areas.

Supplementary Materials: The following are available online at <https://www.mdpi.com/article/10.3390/su14010398/s1>, Figure S1: Representative stereomicroscope pictures of left Sagittal otoliths of *Chelon auratus* examined in the study. Scale bar: 3 mm; Figure S2: Representative stereomicroscope pictures of left Sagittal otoliths of *Chelon labrosus* examined in the study. Scale bar: 3 mm; Figure S3: Representative stereomicroscope pictures of left Sagittal otoliths of *Oedalechilus labeo* examined in the study. Scale bar: 3 mm. Table S4: Chemical parameter of Ganzirri lagoon during the sampling periods.

Author Contributions: Conceptualization, C.D. and G.C.; methodology, S.N., S.F. and M.A.; software, S.F. and S.S.; validation, S.N., C.G. and C.D.; formal analysis, S.S. and S.F.; investigation, C.D. and M.A.; resources, N.S.; data curation, G.L.; writing—original draft preparation, C.D. and S.N.; writing—review and editing, G.C., S.S. and M.A.; visualization, G.P.; supervision, N.S. and G.C.; project administration, N.S. and G.C.; funding acquisition, N.S. and G.C. All authors have read and agreed to the published version of the manuscript.

Funding: This research received no external funding.

Institutional Review Board Statement: Not applicable.

Informed Consent Statement: Not applicable.

Data Availability Statement: Not applicable.

Conflicts of Interest: The authors declare no conflict of interest.

References

1. Schulz-Mirbach, T.; Ladich, F.; Plath, M.; Heß, M. Enigmatic ear stones: What we know about the functional role and evolution of fish otoliths. *Biol. Rev.* **2019**, *94*, 457–482. [[CrossRef](#)] [[PubMed](#)]
2. Flock, Å.; Goldstein, M.H. Cupular movement and nerve impulse response in the isolated semicircular canal. *Brain Res.* **1978**, *157*, 11–19. [[CrossRef](#)]
3. Lowenstein, O.; Roberts, T.D.M. The equilibrium function of the otolith organs of the thornback ray (*Raja clavata*). *J. Physiol.* **1949**, *110*, 392–415. [[CrossRef](#)] [[PubMed](#)]
4. Anken, R.H.; Baur, U.; Hilbig, R. Clinorotation increases the growth of utricular otoliths of developing cichlid fish. *Microgravity Sci. Technol.* **2010**, *22*, 151–154. [[CrossRef](#)]
5. Hawkins, A.D. Underwater sound and fish behaviour. In *Behaviour of Teleost Fishes*; Springer: Boston, MA, USA, 1993; pp. 129–169.
6. v. Frisch, K. Über den Sitz des Geruchsinnes bei Insekten. *Naturwissenschaften* **1922**, *10*, 454–455. [[CrossRef](#)]
7. Fay, R.R. The goldfish ear codes the axis of acoustic particle motion in three dimensions. *Science* **1984**, *225*, 951–954. [[CrossRef](#)]
8. Cermeño, P.; Morales-Nin, B.; Uriarte, A. Juvenile European anchovy otolith microstructure. *Sci. Mar.* **2006**, *70*, 553–557. [[CrossRef](#)]
9. Nolf, D. *Otolithi Piscium. Handbook of Paleichthyology*; Fischer, G., Ed.; Lubrecht & Cramer Ltd.: Port Jervis, NY, USA, 1985; Volume 10.
10. Pannella, G. Fish otoliths: Daily growth layers and periodical patterns. *Science* **1971**, *173*, 1124–1127. [[CrossRef](#)]
11. Campana, S.E. Chemistry and composition of fish otoliths: Pathways, mechanisms and applications. *Mar. Ecol. Prog. Ser.* **1999**, *188*, 263–297. [[CrossRef](#)]
12. Campana, S.E.; Thorrold, S.R. Otoliths, increments, and elements: Keys to a comprehensive understanding of fish populations? *Can. J. Fish. Aquat. Sci.* **2001**, *58*, 30–38. [[CrossRef](#)]
13. Kerr, L.A.; Campana, S.E. Chemical Composition of Fish Hard Parts as a Natural Marker of Fish Stocks. In *Stock Identification Methods: Applications in Fishery Science*, 2nd ed.; Elsevier: San Diego, CA, USA, 2013; pp. 205–234. ISBN 9780123970039.
14. Morales-Nin, B. Review of the growth regulation processes of otolith daily increment formation. *Fish. Res.* **2000**, *46*, 53–67. [[CrossRef](#)]
15. Nolf, D.; de Potter, H.; Lafond-Grellety, J. *Hommage à Joseph Chaine et Jean Duvergier: Diversité et Variabilité des Otolithes des Poissons*; Palaeo Publishing and Library vzw: Mortsel, Belgium, 2009.
16. Tuset, V.M.; Farré, M.; Otero-Ferrer, J.L.; Vilar, A.; Morales-Nin, B.; Lombarte, A. Testing otolith morphology for measuring marine fish biodiversity. *Mar. Freshw. Res.* **2016**, *67*, 1037–1048. [[CrossRef](#)]
17. Tuset, V.M.; Lombarte, A.; Assis, C.A. Otolith atlas for the western Mediterranean, north and central eastern Atlantic. *Sci. Mar.* **2008**, *72*, 7–198. [[CrossRef](#)]
18. Nolf, D. Studies on fossil otoliths—The state of the art. *Recent Dev. Fish. Otolith Res.* **1995**, *19*, 513–544.
19. Lin, C.H.; Girone, A.; Nolf, D. Fish otolith assemblages from Recent NE Atlantic sea bottoms: A comparative study of palaeoecology. *Palaeogeogr. Palaeoclimatol. Palaeoecol.* **2016**, *446*, 98–107. [[CrossRef](#)]
20. Disspain, M.C.F.; Ulm, S.; Gillanders, B.M. Otoliths in archaeology: Methods, applications and future prospects. *J. Archaeol. Sci. Rep.* **2016**, *6*, 623–632. [[CrossRef](#)]
21. D'Iglio, C.; Savoca, S.; Rinelli, P.; Spanò, N. Diet of the Deep-Sea Shark *Galeus melastomus* Rafinesque, 1810, in the Mediterranean Sea: What We Know and What We Should Know. *Sustainability* **2021**, *13*, 3962. [[CrossRef](#)]
22. D'Iglio, C.; Albano, M.; Tiralongo, F.; Famulari, S.; Rinelli, P.; Savoca, S.; Spanò, N.; Capillo, G. Biological and Ecological Aspects of the Blackmouth Catshark (*Galeus melastomus* Rafinesque, 1810) in the Southern Tyrrhenian Sea. *J. Mar. Sci. Eng.* **2021**, *9*, 967. [[CrossRef](#)]
23. Mahé, K.; Evano, H.; Mille, T.; Muths, D.; Bourjea, J. Otolith shape as a valuable tool to evaluate the stock structure of swordfish *Xiphias gladius* in the Indian Ocean. *African J. Mar. Sci.* **2016**, *38*, 457–464. [[CrossRef](#)]
24. Morat, F.; Letourneur, Y.; Nérini, D.; Banaru, D.; Batjakas, I.E. Discrimination of red mullet populations (Teleostean, Mullidae) along multi-spatial and ontogenetic scales within the Mediterranean basin on the basis of otolith shape analysis. *Aquat. Living Resour.* **2012**, *25*, 27–39. [[CrossRef](#)]
25. Vignon, M.; Morat, F. Environmental and genetic determinant of otolith shape revealed by a non-indigenous tropical fish. *Mar. Ecol. Prog. Ser.* **2010**, *411*, 231–241. [[CrossRef](#)]
26. Ramírez-Pérez, J.S.; Quiñónez-Velazquez, C.; García-Rodríguez, F.J.; Félix-Uraga, R.; Melo-Barrera, F.N. Using the shape of Sagitta Otoliths in the discrimination of phenotypic stocks in *Scomberomorus sierra* (Jordan and Starks, 1895). *J. Fish. Aquat. Sci.* **2010**, *5*, 82–93. [[CrossRef](#)]

27. Marengo, M.; Baudouin, M.; Viret, A.; Laporte, M.; Berrebi, P.; Vignon, M.; Marchand, B.; Durieux, E.D.H. Combining microsatellite, otolith shape and parasites community analyses as a holistic approach to assess population structure of *Dentex dentex*. *J. Sea Res.* **2017**, *128*, 1–14. [[CrossRef](#)]
28. Rebaya, M.; Ben Faleh, A.; Allaya, H.; Khedher, M.; Trojette, M.; Marsaoui, B.; Fatnassi, M.; Chalh, A.; Quignard, J.P.; Trabelsi, M. Otolith shape discrimination of *Liza ramada* (Actinopterygii: Mugiliformes: Mugilidae) from marine and estuarine populations in Tunisia. *Acta Ichthyol. Piscat.* **2017**, *47*, 13–21. [[CrossRef](#)]
29. Starrs, D.; Ebner, B.C.; Fulton, C.J. All in the ears: Unlocking the early life history biology and spatial ecology of fishes. *Biol. Rev.* **2016**, *91*, 86–105. [[CrossRef](#)] [[PubMed](#)]
30. McGowan, N.; Fowler, A.M.; Parkinson, K.; Bishop, D.P.; Ganio, K.; Doble, P.A.; Booth, D.J.; Hare, D.J. Beyond the transect: An alternative microchemical imaging method for fine scale analysis of trace elements in fish otoliths during early life. *Sci. Total Environ.* **2014**, *494–495*, 177–186. [[CrossRef](#)] [[PubMed](#)]
31. Izzo, C.; Doubleday, Z.A.; Schultz, A.G.; Woodcock, S.H.; Gillanders, B.M. Contribution of water chemistry and fish condition to otolith chemistry: Comparisons across salinity environments. *J. Fish. Biol.* **2015**, *86*, 1680–1698. [[CrossRef](#)]
32. Lombarte, A.; Tuset, V.M. Chapter3-Morfometría de otolitos. In *Métodos de Estudios con Otolitos: Principios y Aplicaciones/ Métodos de Estudios con Otolitos: Principios e Aplicações*; Volpedo, A.V., Vaz-dos-Santos, A.M., Eds.; PIESECE-SPU: Buenos Aires, Argentina, 2015; p. 31.
33. D'Iglio, C.; Albano, M.; Famulari, S.; Savoca, S.; Panarello, G.; Di Paola, D.; Perdichizzi, A.; Rinelli, P.; Lanteri, G.; Spanò, N.; et al. Intra- and interspecific variability among congeneric *Pagellus* otoliths. *Sci. Rep.* **2021**, *11*, 16315. [[CrossRef](#)]
34. Popper, A.N.; Ramcharitar, J.; Campana, S.E. Why otoliths? Insights from inner ear physiology and fisheries biology. *Mar. Freshw. Res.* **2005**, *56*, 497–504. [[CrossRef](#)]
35. Montanini, S.; Stagioni, M.; Valdrè, G.; Tommasini, S.; Vallisneri, M. Intra-specific and inter-specific variability of the sulcus acusticus of sagittal otoliths in two gurnard species (Scorpaeniformes, Triglidae). *Fish. Res.* **2015**, *161*, 93–101. [[CrossRef](#)]
36. Bolles, K.L.; Begg, G.A. Distinction between silver hake (*Merluccius bilinearis*) stocks in U.S. waters of the northwest Atlantic based on whole otolith morphometrics. *Fish. Bull.* **2000**, *98*, 451–462.
37. Murta, A.G. Morphological variation of horse mackerel (*Trachurus trachurus*) in the Iberian and North African Atlantic: Implications for stock identification. *ICES J. Mar. Sci.* **2000**, *57*, 1240–1248. [[CrossRef](#)]
38. González Castro, M.; Abachian, V.; Perrotta, R.G. Age and growth of the striped mullet, *Mugil platanus* (Actinopterygii, Mugilidae), in a southwestern Atlantic coastal lagoon (37°32'S-57°19'W): A proposal for a life-history model. *J. Appl. Ichthyol.* **2009**, *25*, 61–66. [[CrossRef](#)]
39. González-Castro, M.; Macchi, G.J.; Cousseau, M.B. Studies on reproduction of the mullet *Mugil platanus* Günther, 1880 (Actinopterygii, Mugilidae) from the Mar Chiquita coastal lagoon, Argentina: Similarities and differences with related species. *Ital. J. Zool.* **2011**, *78*, 343–353. [[CrossRef](#)]
40. Whitfield, A.K. Ecological Role of Mugilidae in the Coastal Zone. In *Biology, Ecology and Culture of Grey Mulletts*; CRC Press: Boca Raton, FL, USA, 2015; pp. 334–358. [[CrossRef](#)]
41. Whitfield, A.K.; Panfili, J.; Durand, J.D. A global review of the cosmopolitan flathead mullet *Mugil cephalus* Linnaeus 1758 (Teleostei: Mugilidae), with emphasis on the biology, genetics, ecology and fisheries aspects of this apparent species complex. *Rev. Fish. Biol. Fish.* **2012**, *22*, 641–681. [[CrossRef](#)]
42. Callicó Fortunato, R.; Benedito Durà, V.; Volpedo, A. The morphology of saccular otoliths as a tool to identify different mugilid species from the Northeastern Atlantic and Mediterranean Sea. *Estuar. Coast. Shelf Sci.* **2014**, *146*, 95–101. [[CrossRef](#)]
43. Turan, C.; Gürlek, M.; Ergüden, D.; Yağlıoğlu, D.; Öztürk, B. Systematic status of nine mullet species (mugilidae) in the Mediterranean sea. *Turk. J. Fish. Aquat. Sci.* **2011**, *11*, 315–321. [[CrossRef](#)]
44. Gallardo-Cabello, M.; Espino-Barr, E.; Cabral-Solís, E.G.; Puente-Gómez, M.; García-Boa, A. Study of the otoliths of striped mullet *Mugil cephalus* Linnaeus, 1758 in Mexican Central Pacific. *J. Fish. Aquat. Sci.* **2012**, *7*, 346–363. [[CrossRef](#)]
45. Marin, E.; Baumar, J.; Quintero, A.; Bussière, D.; Dodson, J.J. Reproduction and recruitment of white mullet (*Mugil curema*) to a tropical lagoon (Margarita Island, Venezuela) as revealed by otolith microstructure. *Fish. Bull.* **2003**, *101*, 809–821.
46. Thomson, J.M. The Mugilidae of the world. *Mem. Queensl. Museum* **1997**, *41*, 547–562.
47. Bacheler, N.M.; Wong, R.A.; Buckel, J.A. Movements and Mortality Rates of Striped Mullet in North Carolina. *N. Am. J. Fish. Manag.* **2005**, *25*, 361–373. [[CrossRef](#)]
48. Greenwood, P.H.; Daget, J.; Gosse, J.P.; Thys van den Audenaerde, D.F.E. Check-List of the Freshwater Fishes of Africa. CLOFFA. ORSTOM Paris, MARC Tervuren. 1984. Available online: https://horizon.documentation.ird.fr/exl-doc/pleins_textes/divers13-06/15357.pdf (accessed on 26 December 2021).
49. Cardona, L. Habitat selection by grey mullets (Osteichthyes: Mugilidae) in Mediterranean estuaries: The role of salinity. *Sci. Mar.* **2006**, *70*, 443–455. [[CrossRef](#)]
50. Wheeler, A.; Whitehead, P.J.P.; Bauchot, M.-L.; Hureau, J.-C.; Nielsen, J.; Tortonese, E. Fishes of the North-Eastern Atlantic and the Mediterranean. Vol. 1. *Copeia* **1986**, *1986*, 266. [[CrossRef](#)]
51. Costa, F. *Atlante dei Pesci dei Mari Italiani*; Biblioteca del mare; Ugo Mursia Editore: Milan, Italy, 1991; ISBN 9788842522591.
52. Koutsidi, M.; Moukas, C.; Tzanatos, E. Trait-based life strategies, ecological niches, and niche overlap in the nekton of the data-poor Mediterranean Sea. *Ecol. Evol.* **2020**, *10*, 7129–7144. [[CrossRef](#)]

53. Blanco, S.; Romo, S.; Villena, M.J.; Martínez, S. Fish communities and food web interactions in some shallow Mediterranean lakes. *Hydrobiologia* **2003**, *506–509*, 473–480. [[CrossRef](#)]
54. Manganaro, A.; Pulicanò, G.; Sanfilippo, M. Temporal evolution of the area of Capo Peloro (Sicily, Italy) from pristine site into urbanized area. *Transit. Waters Bull.* **2011**, *5*, 23–31. [[CrossRef](#)]
55. Bottari, A.; Bottari, C.; Carveni, P.; Giacobbe, S.; Spanò, N. Genesis and geomorphologic and ecological evolution of the Ganzirri salt marsh (Messina, Italy). *Quat. Int.* **2005**, *140–141*, 150–158. [[CrossRef](#)]
56. Albano, M.; Panarello, G.; Di Paola, D.; D'Angelo, G.; Granata, A.; Savoca, S.; Capillo, G. The mauve stinger *Pelagia noctiluca* (Cnidaria, Scyphozoa) plastics contamination, the Strait of Messina case. *Int. J. Environ. Stud.* **2021**, *78*, 977–982. [[CrossRef](#)]
57. Savoca, S.; Grifó, G.; Panarello, G.; Albano, M.; Giacobbe, S.; Capillo, G.; Spanó, N.; Consolo, G. Modelling prey-predator interactions in Messina beachrock pools. *Ecol. Modell.* **2020**, *434*, 109206. [[CrossRef](#)]
58. Capillo, G.; Panarello, G.; Savoca, S.; Sanfilippo, M.; Albano, M.; Volsi, R.L.; Consolo, G.; Spanò, N. Intertidal ponds of messina's beachrock faunal assemblage, evaluation of ecosystem dynamics and communities' interactions. *AAPP Atti Accad. Pelorit. Pericol. Cl. Sci. Fis. Mat. Nat.* **2018**, *96*, A41–A416. [[CrossRef](#)]
59. Mazzola, A.; Bergamasco, A.; Calvo, S.; Caruso, G.; Chemello, R.; Colombo, F.; Giaccone, G.; Gianguzza, P.; Guglielmo, L.; Leonardi, M.; et al. Sicilian transitional waters: Current status and future development. *Chem. Ecol.* **2010**, *26*, 267–283. [[CrossRef](#)]
60. Sanfilippo, M. La Componente Organica del Seston nel Lago di Ganzirri: Qualità e Valore Nutrizionale come Risorsa Ambientale. Ph.D. Thesis, University of Messina, Messina, Italy, 2000.
61. Regione Sicilia. *Istituzione della Riserva Naturale Laguna di Capo Peloro, Ricadente nel Comune di Messina*; Regione Sicilia: Messina, Italy, 21 June 2011.
62. Ec. Council Directive 92/43/EEC on the Conservation of Natural Habitats and of Wild Fauna and Flora; European Commission: Bruxelles, Belgium, 1992; Volume L269, pp. 1–15.
63. European Community. *Council Directive of 2 April 1979 on the Conservation of Wild Birds (79/409/EEC)*; European Community: Bruxelles, Belgium, 1979; Volume 94, p. 18.
64. Fischer, W. Fiches FAO d'identification des especes pour les besoins de la peche. (Revision 1). In *Mediterranee et mer Noire. Zone de Peche 37. Vertebres*; FAO: Rome, Italy, 1987.
65. Bauchot, M.-L. Poissons osseux. Fiches FAO d'identification des espèces pour les besoins la pêche. (Révision 1). In *Méditerranée mer Noire. Zone Pêche 37. Vol. II. Vertébrés*; FAO: Rome, Italy, 1987.
66. Spanò, N.; Di Paola, D.; Albano, M.; Manganaro, A.; Sanfilippo, M.; D'Iglio, C.; Capillo, G.; Savoca, S. Growth performance and bioremediation potential of *Gracilaria gracilis* (Steentoft, L.M. Irvine & Farnham, 1995). *Int. J. Environ. Stud.* **2021**, 1–13. [[CrossRef](#)]
67. Follesa, M.C.; Carbonara, P. *Atlas of the Maturity Stages of Mediterranean Fishery Resources. Studies and Reviews N. 99*; FAO: Rome, Italy, 2019; ISBN 9789251319758.
68. Schneider, C.A.; Rasband, W.S.; Eliceiri, K.W. NIH Image to ImageJ: 25 years of image analysis. *Nat. Methods* **2012**, *9*, 671–675. [[CrossRef](#)] [[PubMed](#)]
69. Jawad, L.A.; Sabatino, G.; Ibáñez, A.L.; Andaloro, F.; Battaglia, P. Morphology and ontogenetic changes in otoliths of the mesopelagic fishes *Ceratoscopelus maderensis* (Myctophidae), *Vinciguerria attenuata* and *V. poweriae* (Phosichthyidae) from the Strait of Messina (Mediterranean Sea). *Acta Zool.* **2018**, *99*, 126–142. [[CrossRef](#)]
70. Libungan, L.A.; Pálsson, S. ShapeR: An R package to study otolith shape variation among fish populations. *PLoS ONE* **2015**, *10*, 1–12. [[CrossRef](#)] [[PubMed](#)]
71. Zhuang, L.; Ye, Z.; Zhang, C.; Ye, Z.; Li, Z.; Wan, R.; Ren, Y.; Dou, S.; Wheeler, A.; Whitehead, P.J.P.; et al. Stock discrimination of two insular populations of *diplodus annularis* (Actinopterygii: Perciformes: Sparidae) along the coast of tunisia by analysis of otolith shape. *J. Fish. Biol.* **2015**, *46*, 1–14. [[CrossRef](#)]
72. Bose, A.P.H.; Zimmermann, H.; Winkler, G.; Kaufmann, A.; Strohmeier, T.; Koblmüller, S.; Sefc, K.M. Congruent geographic variation in saccular otolith shape across multiple species of African cichlids. *Sci. Rep.* **2020**, *10*, 1–14. [[CrossRef](#)]
73. Abaad, M.; Tuset, V.M.; Montero, D.; Lombarte, A.; Otero-Ferrer, J.L.; Haroun, R. Phenotypic plasticity in wild marine fishes associated with fish-cage aquaculture. *Hydrobiologia* **2016**, *765*, 343–358. [[CrossRef](#)]
74. Sadighzadeh, Z.; Tuset, V.M.; Valinassab, T.; Dadpour, M.R.; Lombarte, A. Comparison of different otolith shape descriptors and morphometrics for the identification of closely related species of *Lutjanus* spp. from the Persian Gulf. *Mar. Biol. Res.* **2012**, *8*, 802–814. [[CrossRef](#)]
75. Torres, G.J.; Lombarte, A.; Morales-Nin, B. Sagittal otolith size and shape variability to identify geographical intraspecific differences in three species of the genus *Merluccius*. *J. Mar. Biol. Assoc. U. K.* **2000**, *80*, 333–342. [[CrossRef](#)]
76. Gauldie, R.W.; Crampton, J.S. An eco-morphological explanation of individual variability in the shape of the fish otolith: Comparison of the otolith of *Hoplostethus atlanticus* with other species by depth. *J. Fish. Biol.* **2002**, *60*, 1204–1221. [[CrossRef](#)]
77. Sadeghi, R.; Esmaeili, H.R.; Zarei, F.; Reichenbacher, B. Population structure of the ornate goby, *Istigobius ornatus* (Teleostei: Gobiidae), in the Persian Gulf and Oman Sea as determined by otolith shape variation using ShapeR. *Environ. Biol. Fishes* **2020**, *103*, 1217–1230. [[CrossRef](#)]
78. Bose, A.P.H.; Adragna, J.B.; Balshine, S. Otolith morphology varies between populations, sexes and male alternative reproductive tactics in a vocal toadfish *Porichthys notatus*. *J. Fish. Biol.* **2017**, *90*, 311–325. [[CrossRef](#)]

79. Çiçek, E.; Avşar, D.; Yeldan, H.; Manaşirli, M. Comparative morphology of the sagittal otolith of mullet species (Mugilidae) from the Iskenderun Bay, north-eastern Mediterranean. *Acta Biol. Turc.* **2020**, *33*, 219–226.
80. Bauzà Rullan, J. Nueva contribución al conocimiento de los otolitos de peces actuales. *Bolletí Soc. d'Història Nat. Balear.* **1960**, *6*, 49–69.
81. Mahé, K.; MacKenzie, K.; Ider, D.; Massaro, A.; Hamed, O.; Jurado-Ruzafa, A.; Gonçalves, P.; Anastasopoulou, A.; Jadaud, A.; Mytilineou, C.; et al. Directional Bilateral Asymmetry in Fish Otolith: A Potential Tool to Evaluate Stock Boundaries? *Symmetry* **2021**, *13*, 987. [[CrossRef](#)]
82. Mahé, K.; Ider, D.; Massaro, A.; Hamed, O.; Jurado-Ruzafa, A.; Gonçalves, P.; Anastasopoulou, A.; Jadaud, A.; Mytilineou, C.; Elleboode, R.; et al. Directional bilateral asymmetry in otolith morphology may affect fish stock discrimination based on otolith shape analysis. *ICES J. Mar. Sci.* **2019**, *76*, 232–243. [[CrossRef](#)]
83. Raffa, C.; Rizzo, C.; Strous, M.; De Domenico, E.; Sanfilippo, M.; Michaud, L.; Lo Giudice, A. Prokaryotic dynamics in the meromictic coastal Lake Faro (Sicily, Italy). *Diversity* **2019**, *11*, 37. [[CrossRef](#)]
84. Giordani, G.; Viaroli, P.; Swaney, D.P.; Murray, N.C. *Nutrient Fluxes in Transitional Zones of the Italian Coast*; LOICZ: Texel, The Netherlands, 2005.
85. Elsdon, T.S.; Wells, B.K.; Campana, S.E.; Gillanders, B.M.; Jones, C.M.; Limburg, K.E.; Secor, D.H.; Thorrold, S.R.; Walther, B.D. Otolith chemistry to describe movements and life-history parameters of fishes: Hypotheses, assumptions, limitations and inferences. In *Oceanography and Marine Biology*; CRC Press: Boca Raton, FL, USA, 2008; Volume 46, pp. 297–330. ISBN 0429137257.
86. Campana, S.E.; Gagne, J.A.; McLaren, J.W. Elemental fingerprinting of fish otoliths using ID-ICPMS. *Mar. Ecol. Prog. Ser.* **1995**, *122*, 115–120. [[CrossRef](#)]
87. Vrdoljak, D.; Matic-Skoko, S.; Peharda, M.; Uvanović, H.; Markulin, K.; Mertz-Kraus, R. Otolith fingerprints reveals potential pollution exposure of newly settled juvenile *Sparus aurata*. *Mar. Pollut. Bull.* **2020**, *160*, 111695. [[CrossRef](#)]
88. Capoccioni, F.; Costa, C.; Aguzzi, J.; Menesatti, P.; Lombarte, A.; Ciccotti, E. Ontogenetic and environmental effects on otolith shape variability in three Mediterranean European eel (*Anguilla anguilla*, L.) local stocks. *J. Exp. Mar. Bio. Ecol.* **2011**, *397*, 1–7. [[CrossRef](#)]
89. Loeppky, A.R.; Belding, L.D.; Quijada-Rodriguez, A.R.; Morgan, J.D.; Pracheil, B.M.; Chakoumakos, B.C.; Anderson, W.G. Influence of ontogenetic development, temperature, and pCO₂ on otolith calcium carbonate polymorph composition in sturgeons. *Sci. Rep.* **2021**, *11*, 1–10. [[CrossRef](#)] [[PubMed](#)]
90. Matic-Skoko, S.; Peharda, M.; Vrdoljak, D.; Uvanović, H.; Markulin, K. Fish and Sclerochronology Research in the Mediterranean: Challenges and Opportunities for Reconstructing Environmental Changes. *Front. Mar. Sci.* **2020**, *7*, 195. [[CrossRef](#)]
91. Matic-Skoko, S.; Vrdoljak, D.; Uvanović, H.; Pavičić, M.; Tutman, P.; Bojanić Varezić, D. Early evidence of a shift in juvenile fish communities in response to conditions in nursery areas. *Sci. Rep.* **2020**, *10*, 1–16. [[CrossRef](#)]
92. Lombarte, A.; Lleonart, J. Otolith size changes related with body growth, habitat depth and temperature. *Environ. Biol. Fishes* **1993**, *37*, 297–306. [[CrossRef](#)]
93. Aguirre, H.; Lombarte, A. Ecomorphological comparisons of sagittae in *Mullus barbatus* and *M. surmuletus*. *J. Fish. Biol.* **1999**, *55*, 105–114. [[CrossRef](#)]
94. Torres, G.J.; Lombarte, A.; Morales-Nin, B. Variability of the sulcus acusticus in the sagittal otolith of the genus *Merluccius* (Merlucciidae). *Fish. Res.* **2000**, *46*, 5–13. [[CrossRef](#)]
95. Volpedo, A.; Diana Echeverría, D. Ecomorphological patterns of the sagitta in fish on the continental shelf off Argentina. *Fish. Res.* **2003**, *60*, 551–560. [[CrossRef](#)]
96. Cruz, A.; Lombarte, A. Otolith size and its relationship with colour patterns and sound production. *J. Fish. Biol.* **2004**, *65*, 1512–1525. [[CrossRef](#)]
97. Stransky, C.; Murta, A.G.; Schlickeisen, J.; Zimmermann, C. Otolith shape analysis as a tool for stock separation of horse mackerel (*Trachurus trachurus*) in the Northeast Atlantic and Mediterranean. *Fish. Res.* **2008**, *89*, 159–166. [[CrossRef](#)]
98. Popper, A.N.; Lu, Z. Structure-function relationships in fish otolith organs. *Fish. Res.* **2000**, *46*, 15–25. [[CrossRef](#)]
99. Jaramilo, A.M.; Tombari, A.D.; Benedito Dura, V.; Eugeni Rodrigo, M.; Volpedo, A.V. Otolith eco-morphological patterns of benthic fishes from the coast of Valencia (Spain). *Thalassas* **2014**, *30*, 57–66.
100. Turan, C.; Caliskan, M.; Kucuktas, H. Phylogenetic relationships of nine mullet species (Mugilidae) in the Mediterranean Sea. *Hydrobiologia* **2005**, *532*, 45–51. [[CrossRef](#)]
101. Durand, J.D.; Shen, K.N.; Chen, W.J.; Jamandre, B.W.; Blel, H.; Diop, K.; Nirchio, M.; Garcia de León, F.J.; Whitfield, A.K.; Chang, C.W.; et al. Systematics of the grey mullets (Teleostei: Mugiliformes: Mugilidae): Molecular phylogenetic evidence challenges two centuries of morphology-based taxonomy. *Mol. Phylogenet. Evol.* **2012**, *64*, 73–92. [[CrossRef](#)] [[PubMed](#)]
102. Papatotriopoulos, V.; Klossa-Kilia, E.; Kiliadis, G.; Alahiotis, S. Genetic divergence and phylogenetic relationships in grey mullets (Teleostei: Mugilidae) based on PCR-RFLP analysis of mtDNA segments. *Biochem. Genet.* **2002**, *40*, 71–86. [[CrossRef](#)] [[PubMed](#)]
103. Cardinale, M.; Doering-Arjes, P.; Kastowsky, M.; Mosegaard, H. Effects of sex, stock, and environment on the shape of known-age Atlantic cod (*Gadus morhua*) otoliths. *Can. J. Fish. Aquat. Sci.* **2004**, *61*, 158–167. [[CrossRef](#)]
104. Simoneau, M.; Casselman, J.M.; Fortin, R. Determining the effect of negative allometry (length/height relationship) on variation in otolith shape in lake trout (*Salvelinus namaycush*), using Fourier-series analysis. *Can. J. Zool.* **2000**, *78*, 1597–1603. [[CrossRef](#)]
105. Monteiro, L.R.; Di Benedetto, A.P.M.; Guillermo, L.H.; Rivera, L.A. Allometric changes and shape differentiation of sagitta otoliths in sciaenid fishes. *Fish. Res.* **2005**, *74*, 288–299. [[CrossRef](#)]

106. Hüseyin, K. Otolith shape in juvenile cod (*Gadus morhua*): Ontogenetic and environmental effects. *J. Exp. Mar. Bio. Ecol.* **2008**, *364*, 35–41. [[CrossRef](#)]
107. Gauldie, R.W. Polymorphic crystalline structure of fish otoliths. *J. Morphol.* **1993**, *218*, 1–28. [[CrossRef](#)]
108. Schulz-Mirbach, T.; Riesch, R.; García de León, F.J.; Plath, M. Effects of extreme habitat conditions on otolith morphology—a case study on extremophile livebearing fishes (*Poecilia mexicana*, *P. sulphuraria*). *Zoology* **2011**, *114*, 321–334. [[CrossRef](#)]
109. Béarez, P.; Carlier, G.; Lorand, J.P.; Parodi, G.C. Destructive and non-destructive microanalysis of biocarbonates applied to anomalous otoliths of archaeological and modern sciaenids (Teleostei) from Peru and Chile. *Comptes Rendus-Biol.* **2005**, *328*, 243–252. [[CrossRef](#)]
110. Falini, G.; Fermani, S.; Vanzo, S.; Miletic, M.; Zaffino, G. Influence on the formation of aragonite or vaterite by otolith macromolecules. *Eur. J. Inorg. Chem.* **2005**, *2005*, 162–167. [[CrossRef](#)]
111. Parmentier, E.; Cloots, R.; Warin, R.; Henrist, C. Otolith crystals (in Carapidae): Growth and habit. *J. Struct. Biol.* **2007**, *159*, 462–473. [[CrossRef](#)]
112. Wilcox Freiburg, E.D. Exploring the Link between Otolith Growth and Function along the Biological Continuum in the Context of Ocean Acidification. Ph.D. Thesis, University of Massachusetts Boston, Boston, MA, USA, 2014.
113. Pikuta, E.V. *Desulfonatronum lacustre* gen. nov., sp. nov.: A new alkaliphilic sulfate-reducing bacterium utilizing ethanol. *Mikrobiologiya* **1998**, *67*, 123–131.
114. Aloisi, G.; Gloter, A.; Krüger, M.; Wallman, K.; Guyot, F.; Zuddas, P. Nucleation of calcium carbonate on bacterial nanoglobules. *Geology* **2006**, *34*, 1017–1020. [[CrossRef](#)]
115. Schulz-Mirbach, T.; Götz, A.; Griesshaber, E.; Plath, M.; Schmahl, W.W. Texture and nano-scale internal microstructure of otoliths in the atlantic molly, *poecilia mexicana*: A high-resolution EBSD study. *Micron* **2013**, *51*, 60–69. [[CrossRef](#)] [[PubMed](#)]
116. Beck, M.; Heck, K.; Able, K.; Bioscience, D.C.-; 2001, U. The identification, conservation, and management of estuarine and marine nurseries for fish and invertebrates: A better understanding of the habitats that serve as. *Bioscience* **2001**, *51*, 633–641. [[CrossRef](#)]
117. Cowen, R.K.; Lwiza, K.M.M.; Sponaugle, S.; Paris, C.B.; Olson, D.B. Connectivity of marine populations: Open or closed? *Science* **2000**, *287*, 857–859. [[CrossRef](#)] [[PubMed](#)]
118. Houde, E.D. Comparative growth, mortality, and energetics of marine fish larvae: Temperature and implied latitudinal effects. *Fish. Bull.* **1989**, *87*, 471–495.
119. Matić-Skoko, S.; Peharda, M.; Pallaoro, A.; Frančević, M. Species composition, seasonal fluctuations, and residency of inshore fish assemblages in the Pantan estuary of the eastern middle Adriatic. *Acta Adriat.* **2005**, *46*, 201–212.
120. Dulčić, J.; Matić-Skoko, S.; Kraljević, M.; Fencil, M.; Glamuzina, B. Seasonality of a fish assemblage in shallow waters of Duće-Glava, eastern middle Adriatic. *Cybium* **2005**, *29*, 57–63.
121. Dulčić, J.; Matić, S.; Kraljević, M. Shallow coves as nurseries for non-resident fish: A case study in the eastern middle Adriatic. *J. Mar. Biol. Assoc. U. K.* **2002**, *82*, 991–993. [[CrossRef](#)]